



Swansea University
Prifysgol Abertawe



Cronfa - Swansea University Open Access Repository

This is an author produced version of a paper published in:
Nature Ecology & Evolution

Cronfa URL for this paper:
<http://cronfa.swan.ac.uk/Record/cronfa48648>

Paper:

Yang, Q., Fowler, M., Jackson, A. & Donohue, I. (2019). The predictability of ecological stability in a noisy world.
Nature Ecology & Evolution, 3(2), 251-259.
<http://dx.doi.org/10.1038/s41559-018-0794-x>

This item is brought to you by Swansea University. Any person downloading material is agreeing to abide by the terms of the repository licence. Copies of full text items may be used or reproduced in any format or medium, without prior permission for personal research or study, educational or non-commercial purposes only. The copyright for any work remains with the original author unless otherwise specified. The full-text must not be sold in any format or medium without the formal permission of the copyright holder.

Permission for multiple reproductions should be obtained from the original author.

Authors are personally responsible for adhering to copyright and publisher restrictions when uploading content to the repository.

<http://www.swansea.ac.uk/library/researchsupport/ris-support/>

1 **The predictability of ecological stability in a noisy world**

2
3 QIANG YANG^{1,2}, MIKE S. FOWLER³, ANDREW L. JACKSON¹, IAN DONOHUE¹

4
5 ¹*Department of Zoology, School of Natural Sciences, Trinity College Dublin, Ireland*

6 ²*Department of Biology, University of Konstanz, Konstanz, Germany*

7 ³*Department of Biosciences, Swansea University, Wales, UK*

8
9 **Running head:** Ecological stability in a stochastic world

10
11 **Keywords:** environmental stochasticity, recovery time, variability, resistance,
12 resilience, autocorrelation, asynchrony, disturbance, perturbation, food-web.

13
14 **Author Contributions:** QY, ID, AJ and MF designed the research. QY performed the
15 numerical simulations and analysed the data. QY and ID drafted the text. All authors
16 contributed to the writing of the manuscript.

17
18 **Email addresses:** qyang@tcd.ie, m.s.fowler@swansea.ac.uk, JACKSOAN@tcd.ie,
19 ian.donohue@tcd.ie

20 **Random environmental variation, or stochasticity, is a key determinant of ecological**
21 **dynamics. While we have some appreciation of how environmental stochasticity can**
22 **moderate the variability and persistence of communities, we know little about its**
23 **implications for the nature and predictability of ecological responses to large**
24 **perturbations. Here, we show that shifts in the temporal autocorrelation (colour) of**
25 **environmental noise provoke trade-offs in ecological stability across a wide range of**
26 **different food-web structures by stabilizing dynamics in some dimensions, while**
27 **simultaneously destabilizing them in others. Specifically, increasingly positive**
28 **autocorrelation (reddening) of environmental noise increases resilience by hastening**
29 **recovery of food-webs following a large perturbation, but reduces their resistance to**
30 **perturbation and increases their temporal variability (reduces biomass stability). In**
31 **contrast, all stability dimensions become less predictable, showing increased variability**
32 **around the mean response, as environmental noise reddens. Moreover, we found**
33 **environmental reddening to be a considerably more important determinant of stability**
34 **than intrinsic food-web characteristics. These findings reveal the fundamental and**
35 **dominant role played by environmental stochasticity in determining the dynamics and**
36 **stability of ecosystems and extend our understanding of how the multiple dimensions of**
37 **stability relate to each other beyond simple white noise environments.**

38 Predicting how ecosystems will respond to global environmental change has become a
39 central focus of ecological research¹⁻⁷. Prediction of ecological responses typically involves
40 the use of static approaches that focus on mean levels of environmental change, such as
41 warming and deforestation^{8,9}. Many approaches overlook environmental stochasticity, which
42 introduces uncertainties and, even when incorporated, is usually considered as a purely
43 random term. However, stochasticity has structure and comprises a key determinant of the
44 dynamics and structure of populations and communities^{10,11}. Exploration of its underlying
45 characteristics, such as its variance and temporal or spectral structure¹²⁻¹⁴, reveals, for
46 example, the frequency and duration of extreme events and determines the variability and

47 persistence of populations^{8,15-21}. For example, Ruokolainen et al.¹³ reviewed how predictable
48 outcomes for population variation depend on the interplay between population density
49 dependence (*i.e.* under-, over-, or purely compensatory dynamics) and the structure of the
50 autocorrelation in environmental stochasticity. Briefly, red noise (positive autocorrelation) is
51 expected to be amplified at the population level in (deterministically) slow growing
52 (undercompensatory) populations, but dampened in rapidly growing (overcompensatory)
53 populations, and *vice versa* for blue noise (negative autocorrelation). However, in spite of its
54 overarching influence on population and community dynamics, the role played by
55 environmental stochasticity in moderating ecological responses to other perturbations,
56 particularly large perturbations, remains mostly unknown.

57 Ecological stability is a multidimensional concept that tries to capture the different
58 aspects of the dynamics of the system and its response to perturbations^{9,22,23}. The concept is
59 fundamental to the conservation and management of natural resources⁹ and has been a central
60 focus of ecological research for decades²³⁻²⁵. The various dimensions of stability, such as the
61 *variability* of community biomass in time and space, and the *resistance* and *resilience* of
62 communities – their capacity to, respectively, resist and recover from perturbations – have,
63 however, typically been considered in isolation, due in part to the difficulty of quantifying
64 them simultaneously in the natural world⁹. Moreover, their behaviour and predictability likely
65 depend strongly on the spatiotemporal range across which they are estimated²⁶. Stability
66 components such as variability and persistence – the length of time a system maintains the
67 same state before it changes in some defined way²³ – are usually estimated from long-term
68 dynamics and are therefore more likely to reflect key features of environmental stochasticity.
69 In contrast, stability components that describe the responses of communities to distinct
70 perturbations, such as resistance and resilience, are determined within shorter time windows.
71 They are consequently likely to be sensitive to the timing and duration of potential extreme
72 events. This makes them less predictable – *i.e.*, they show greater variation around the mean
73 community response. Nonetheless, their general response pattern can be still revealed by

74 examining and averaging the stability of many similar systems experiencing the same
75 environmental perturbations.

76 Here, we explore how three key components of ecological stability (Fig. 1) – recovery
77 time (the reciprocal of resilience), the extent of change in community structure in response to
78 perturbation (a measure of resistance; larger extent of change indicates weak resistance^{22,23}),
79 and variability – are regulated by environmental stochasticity. We use simulated model food-
80 webs described by the general Lotka-Volterra system²⁷⁻²⁹ to examine both the responses and
81 predictability of these stability components along gradients of the key factors that characterise
82 environmental stochasticity – its temporal autocorrelation [*i.e.* its *colour*^{14,20}] and the
83 correlations in species responses to it^{13,14,20,21,30}. As predators tend to be particularly important
84 drivers of community dynamics and, consequently, predator loss is considered as one of the
85 most profound biotic perturbations that can occur^{7,31-33}, we perturbed our model systems by
86 reducing the densities of the apex predator in each food-web by 50%, as a single pulse
87 perturbation, coupled with short-term, continuously fluctuating coloured environmental
88 variation.

89 Given the significant disjoint between many theoretical measures of stability and what
90 can be measured empirically⁹, we quantified all components of stability empirically across a
91 broad range of four-species food-web modules (Supplementary Fig. 1, including, for
92 example, simple food chains, modules including omnivory and / or apparent competition) –
93 subnetworks of tightly interacting species that act as the ‘building blocks’ of food-webs³⁴⁻³⁶ –
94 to explore the generality of our findings. Our results revealed highly consistent patterns across
95 all types of food webs explored and demonstrate contrasting patterns across different stability
96 dimensions and increasing uncertainty in community responses under redder environments.

97

98 **Results**

99 To illustrate our findings, we focus initially on the effect of temporal autocorrelation on
100 the dynamics of one randomly assembled community, from what is the simplest food-web
101 module – the food chain (*i.e.*, Module 1 in Supplementary Fig. 1). We then expand our focus
102 to 100 replicate communities from each of 14 food-web modules to explore the generality of
103 our results (Supplementary Fig. 1).

104 Increased temporal autocorrelation (reddening) of environmental stochasticity both
105 stabilized and destabilized the example food chain community along different dimensions of
106 stability (Fig 2a). Increasing autocorrelation from negative (blue) to positive (red)
107 destabilized the community by increasing both total biomass variability and the extent of
108 change in community structure (*i.e.* reducing resistance) in response to the initial, large
109 perturbation. Simultaneously, environmental reddening enhanced stability by reducing
110 recovery time after the perturbation (*i.e.* increasing resilience; Fig. 2a). In contrast, the
111 uncertainty (coefficient of variation) in all stability responses increased consistently with
112 environmental reddening (Fig. 2b), indicating that higher temporal autocorrelation reduces the
113 predictability of ecological stability, at the scale of individual food web responses.

114 Results from the example food chain community were consistent not only with those
115 from the other communities with the same module structure, but also with those from across
116 all other modules examined (Fig. 3). Recovery time decreased with environmental reddening,
117 while the extent of community change and biomass variability both increased (Fig. 3a).
118 Further, the predictability of all dimensions of stability decreased monotonically as
119 environmental autocorrelation increased, as the uncertainty (coefficient of variation) across
120 individual food web responses more than doubled in every case as noise colour changed from
121 blue to red (Fig. 3b).

122 The correlation in species responses to environmental fluctuations modified the specific
123 response of both recovery time and variability, but had little effect on the extent of
124 community change (Fig. 4a). When correlations in species responses to environmental
125 fluctuations were weak, communities showed lower biomass variability (*i.e.* increased

126 stability) compared to when they were strong. However, weaker correlations in species
127 environmental responses simultaneously destabilized communities by increasing recovery
128 time compared to when they were strong (Fig. 4a). There was no general effect of correlations
129 in species-environment responses on the uncertainty of any of the stability components (Fig.
130 4b).

131 Variation in the general response of all stability components analysed was almost
132 entirely accounted for by the explanatory variables included in our random forest regression
133 models (pseudo- R^2 values ≥ 0.98 in every case; Fig. 5a). However, the models accounted for
134 significantly lower variation in the specific responses of stability components to distinct runs
135 of stochastic noise (regression pseudo- R^2 of recovery time, extent of community change and
136 variability was reduced to, respectively, 0.38, 0.35 and 0.72; Fig. 5a). These reductions in
137 explanatory power were particularly acute for resistance and resilience, consistent with the
138 high uncertainty associated with these stability components in previous analyses (Figs. 2b and
139 Fig. 3b).

140 The temporal autocorrelation of environmental stochasticity was the dominant
141 determinant of both the general and specific responses of all stability components examined
142 (Fig. 5b). Species environmental response correlations had a far weaker effect on stability
143 dimensions than temporal autocorrelation, and contributed little to the general response of any
144 stability component, though they had some influence on the specific temporal response of
145 communities in terms of their recovery time and variability (Fig 5b). Compared to these
146 components of environmental stochasticity, both community and module characteristics were
147 of minor importance in determining stability (Fig. 5b).

148

149 **Discussion**

150 Although environmental stochasticity plays a critical role in determining the assembly,
151 diversity, evolution, and functioning of ecological communities^{13,30,37,38}, it is commonly
152 treated as synonymous with fundamental unpredictability. In contrast, our results demonstrate

153 that key aspects of environmental stochasticity can regulate ecological stability responses in a
154 predictable way. Within the given range of the parameters of our models, we identified the
155 two key factors that characterise stochasticity – its temporal autocorrelation and the
156 correlations in species responses to it – as more important determinants of ecological stability
157 than any inherent characteristics of community or module structure. Moreover, we found that
158 the effects of environmental stochasticity on the responses and uncertainties associated with
159 different components of ecological stability are highly consistent across a large variety of
160 food-web structures. These findings highlight the fundamental importance of applying
161 environmental stochasticity to illuminate our understanding of – and enhance significantly our
162 capacity to predict – the different dimensions of ecological stability in communities.

163 Shifts in both the temporal autocorrelation of environmental noise and correlations of
164 species responses to it provoked trade-offs among components of stability by stabilizing
165 communities in some ways but simultaneously destabilizing them in others. The reddening of
166 environmental noise reduced recovery time (*i.e.* increasing resilience), while simultaneously
167 increasing both the extent of change in response to perturbation (*i.e.* reducing resistance) and
168 variability. Moreover, these effects were amplified when correlations in species responses to
169 environmental fluctuations were strong. In general, as was the case in our study, increasing
170 environmental reddening amplifies the fluctuations in population density in under-
171 compensatory populations^{13,39,40}. Increases in both variability and the extent of change in
172 response to perturbation was a consequence of the propagation of this enlarged population
173 (and community) variance as environmental stochasticity reddened. Further, the higher
174 temporal variability of both populations and communities in red noise environments more
175 rapidly overwhelmed the effect of the initial perturbation, bringing the perturbed and
176 unperturbed communities into more similar stochastic biomass envelopes (the shaded bands
177 in Fig. 1b) with the same environmental stochasticity, consequently reducing recovery time.
178 Increasing correlations of species responses to environmental noise enhanced this effect
179 further by increasing species synchrony, which reduces the buffering effect caused by species
180 responding in more diverse ways to environmental fluctuations⁴¹⁻⁴⁴.

181 Our findings highlight the challenges in predicting ecological stability on local
182 temporal and spatial scales. Despite the trade-off that occurred among components of stability
183 as temporal autocorrelation changed, their uncertainty increased consistently as
184 environmental noise reddened. When environmental colour changes from blue through white
185 to red, populations experience longer runs of extreme conditions⁴⁰. As undercompensatory
186 populations are slow to track environmental change, longer runs of extreme conditions are
187 then translated into longer runs of low (or high) total biomass densities. The increase in the
188 duration of extreme runs increases the variability of recovery time as long runs of good
189 environmental conditions reduce recovery time by helping the community recover quickly
190 from the initial large perturbation, while long runs of poor environmental conditions increase
191 recovery time by making it harder for the community to return to the equilibrium envelope.
192 Likewise, long runs of poor environmental conditions will tend to amplify the initial large
193 perturbation more than long runs of good conditions (which will tend to cancel it out quickly,
194 bringing the community back to the equilibrium envelope). This means that, under a run of
195 poor conditions, the extent of community change will be larger under red than under
196 blue/white noise as the poor conditions drag the initial perturbation further from the
197 equilibrium envelope, while under a long run of good conditions, the community is taken less
198 far from the equilibrium envelope than under blue/white noise. All these together resulted in
199 higher uncertainty, and thus lower predictability, in the extent of community change under red
200 than under blue/white noise.

201 Our results also show that recovery time and resistance are much more difficult to
202 predict than biomass variability. This is likely a consequence of the difference in time ranges
203 across which these different dimensions of stability are quantified. Resistance and recovery
204 time were quantified from discrete time points within a relatively short time window. Over
205 increasingly short time ranges, the relative importance of distinct patterns in the timing and
206 duration of a few individual extreme events across the (50) different replicate runs of
207 environmental stochasticity is enhanced, reducing the ratio of signal to noise, and leading to a
208 large variance in resistance and recovery time among replicates. In contrast, biomass

209 variability was measured across the whole simulation time, which is likely to reflect
210 stochastic structure much more closely as the effects of multiple individual extreme events are
211 averaged out. Consistent with this, shortening the time window over which variability was
212 quantified increased its uncertainty significantly (Supplementary Fig. 2). This mechanism is
213 also likely to be responsible for the lack of importance of species environmental response
214 correlations in determining the extent of community change in response to perturbation. Over
215 the relatively short time periods that the extent of community change was measured, the
216 impact of the single, large perturbation overwhelmed any effect that correlations of species
217 environmental responses could exert on this stability dimension.

218 The complex and hierarchical nature of ecology provides a key challenge for predicting
219 ecological stability in stochastic environments. For simplicity, we used four-species food-web
220 modules as the basic structure of the biological community. Although these include some of
221 the most common building blocks of the ecological networks found in nature³⁴⁻³⁶ and have
222 been used broadly to study ecological stability and both environmental and demographic
223 stochasticity, they nonetheless omit some important biological details that are could affect
224 how biological communities respond to environmental stochasticity. For example,
225 demographic stochasticity and variation in realised vital rates through age, stage, genetic,
226 behavioural, spatial or other biological structure can all modify population responses to
227 environmental variation¹¹. These factors may be either affected directly by environmental
228 stochasticity or may regulate the impact of environmental stochasticity on other biological or
229 ecological characteristics. For example, our models assume the interaction coefficient a_{ij} to be
230 constant (*i.e.* consumption by consumers increases linearly across all prey densities, similar to
231 Holling's type I functional response). In nature, depending on the body size ratio between the
232 consumer and the resource species, consumers may follow type I, II or III functional response
233 patterns⁴⁵. Though the choice of functional response curve could influence system dynamics,
234 we would nonetheless expect qualitatively similar shifts in the stability characteristics of the
235 system with changes in the temporal autocorrelation of environmental noise (Supplementary
236 Table 1; see also Kaneryd *et al.*⁴⁶). While including all the biological complexities we

237 describe above together with environmental stochasticity would result in a highly complex
238 model, incorporating a subset of the biological details in the proper candidate stochastic
239 model may reveal the interplay between key biological details and environmental
240 stochasticity in determining ecological stability. For example, the Allometric-Trophic-
241 Network (ATN) model⁴⁷ may reveal how environmental stochasticity affects ecological
242 stability through regulation of metabolic rates, either through direct regulation of the
243 metabolic rate or indirect regulation via changing the body mass/size of individuals.

244 In our study, all three stability measures are based on the assumption of the existence of
245 a unique stable-point equilibrium in the food-webs, and our community assembly process
246 ensured that this was the case. Ecosystems can, however, shift from one stable state to another
247 type of equilibrium as a consequence of either strong environmental forcing or positive
248 feedback from the system^{24,48}. Environmental stochasticity may prevent the community from
249 arriving at its deterministic equilibrium in at least three ways. First, for a deterministic system
250 prone to bifurcation or chaos, the existence of environmental stochasticity will inevitably
251 increase the unpredictability of the system's dynamics in some way. Second, as slow trackers
252 of environmental change, undercompensatory populations may present strong positive
253 autocorrelation in their dynamics under red noise, and may therefore be more prone to regime
254 shifts⁴⁹. Third, sufficiently large environmental stochasticity can cause the community to
255 fluctuate around its equilibrium – either a stable point or a limit cycle – within a characteristic
256 distribution. In systems close to a bifurcation boundary, stochasticity can cause the system to
257 appear to switch to a qualitatively different type of dynamical behaviour, such as from
258 fluctuating around a stable point equilibrium to fluctuating around a cycle⁵⁰. The deterministic
259 negative feedback inherent in consumer-resource interactions can, for example, make these
260 systems prone to cycling⁵¹. When the cycles are transient (*i.e.* damped oscillations), systems
261 will settle onto a point equilibrium in the absence of stochasticity. With stochasticity,
262 however, the same systems may exhibit sustained cycles⁵⁰. In this way, stochasticity can
263 provoke qualitatively different dynamics in ecosystems that would not otherwise be apparent.

264 For simplicity and tractability, we controlled the variance of environmental
265 stochasticity at the same level, and assigned set levels of species response correlations to
266 environmental fluctuations for all consumers and basal species, whose populations all exhibit
267 undercompensatory dynamics. In nature, communities consist of both overcompensatory and
268 undercompensatory populations, each of which could respond in different ways to
269 environmental stochasticity. Moreover, different species experience different levels of
270 stochasticity across multiple environmental factors all the time. These complexities may scale
271 up to affect ecosystem stability by propagation through the linear, nonlinear, and higher-order
272 interactions⁵² between the other components of the system. Predicting the outcomes of these
273 processes is a complex challenge. However, our findings demonstrate that incorporating key
274 characteristics of environmental stochasticity into our models is an essential step towards
275 improving prediction in ecological systems. Moreover, understanding how different elements
276 of human-induced global environmental change modifies the temporal and spatial
277 autocorrelation of environmental noise is necessary to provide improved understanding and
278 prediction of ecosystem stability.

279

280 **Methods**

281 *Food-web construction and simulations*

282 We constructed sets of 14 distinct four-species food web modules (Supplementary Fig.
283 1) to cover a large range of different network structures that vary in both trophic topology and
284 connectance. We then constructed 100 individual communities within each set of module
285 structures. The dynamics of our modules are described by the general Lotka-Volterra
286 system²⁷⁻²⁹:

$$287 \quad \frac{dN_i(t)}{dt} = N_i(t) \left(r_i + \sum_{j=1}^4 a_{ij} N_j(t) + \varepsilon_i(t) \right) \quad (1)$$

288 where i and j are the identity of species in the community, N_i is the population density of
289 species i , r_i is the intrinsic growth/mortality rate (positive for basal species, otherwise

290 negative), a_{ij} is the interaction coefficient that describes the per capita effect of the j^{th} species
291 on the growth/mortality rate of the i^{th} species (positive if it enhances population growth;
292 negative if it causes decreases in growth) and $\varepsilon_i(t)$ is the species-specific response to
293 environmental stochasticity (see below).

294 We followed Petchey *et al.*²⁹ to parameterize the models. We first set the growth rates
295 of basal species to 1, and drew mortality rates (*i.e.* the intrinsic rate of change in the absence
296 of resources and predation) of consumers randomly from a uniform distribution. Petchey *et*
297 *al.*²⁹ drew mortality rates from [-0.001, 0]. As our food-web modules have fewer species but
298 more trophic levels, we drew mortality rates from [-0.001, -0.1] instead to avoid extremely
299 small mortality rates of consumers, particularly the top consumer. We sorted the mortality
300 rate so that the predator had lower mortality rates than their prey, as species at higher trophic
301 levels tend to be larger⁵³ and large size generally leads to greater longevity and low mortality
302 rates^{54,55}. The value of the *per capita* effect of the consumer on its resources a_{ij} was assigned
303 depending on the number of resource species. When the consumer fed on only one species, a_{ij}
304 was set to 0.5. Otherwise, a randomly chosen link was given one strong interaction coefficient
305 (set to 0.4), and other links were assigned weak interactions and set to 0.1 divided by the
306 number of the resources minus 1. This approach resulted in a skewed distribution of
307 interaction strengths, which is commonly found in real ecological networks^{56,57}. The *per*
308 *capita* effect of the resource species on its consumer a_{ji} was calculated as a_{ij} times the
309 conversion efficiency. We set the conversion efficiency of non-omnivorous links to 0.2 and
310 that of omnivorous links to 0.02 by assuming that it takes more mass of the basal species
311 (plants in most situations) than animals to produce one predator offspring²⁹. Intraspecific
312 competition occurred in all species and was set to 1 for basal species and 0.1 for other species.
313 Interspecific competition among basal species was modelled by setting the appropriate
314 competition coefficients (drawn randomly from the uniform distribution [0, 0.5]).
315 Interspecific competition among consumer species was indirect through consumption of
316 shared resources²⁹.

317 Using the interaction coefficient matrix \mathbf{A} , with entries a_{ij} , and the vector \mathbf{R} , with
318 entries of r_i , we estimated the density of species at equilibrium, N_i^* . At equilibrium, the *per*
319 *capita* change rate of all species is zero, so $\mathbf{A}\mathbf{N}^* = -\mathbf{R}$. Then, \mathbf{N}^* can be solved as $\mathbf{N}^* = -\mathbf{A}^{-1}\mathbf{R}$,
320 where \mathbf{A}^{-1} is the inverse of matrix \mathbf{A} . The equilibrium Jacobian interaction matrix \mathbf{J}^* (also
321 known as the community matrix) with entries J_{ij} , which is used to test the local stability of the
322 constructed community²⁵, is $J_{ij} = a_{ij}N_i^*$. When the maximum real part of the dominant
323 eigenvalue of the community matrix is negative, the deterministic system will settle to a
324 stable point equilibrium. However, if this negative eigenvalue is close to zero, the system
325 approaches a bifurcation threshold. To ensure against alternative full coexisting stable states
326 (*e.g.*, limit cycles or chaotic fluctuations) by stochastic resonance, we excluded communities
327 whose maximum real part of the dominant eigenvalues was larger than -0.005 (see
328 Supplementary Fig. 3 for the realised distributions of the maximum real part of the
329 eigenvalues from our model communities). This is sufficiently far from the bifurcation
330 threshold to avoid the system shifting to another dynamical attractors under the stochastic
331 variation we considered. The process of parameterization continued until, for each of the 14
332 food-web modules, we constructed 100 communities that satisfied the requirements of both
333 local stability and feasibility⁵⁸⁻⁶⁰. The equilibrium species densities of communities generated
334 by this method conformed to the pyramidal structure, with species of lower trophic levels
335 being more abundant (Supplementary Fig. 4).

336

337 *Environmental stochasticity*

338 The effect of environmental stochasticity was incorporated in the dynamical system of
339 Equation (1) by the continuous variable $\varepsilon_i(t)$, which represents the specific response to
340 environmental stochasticity. When the time step is small, $\varepsilon_i(t)$ can be approximately
341 represented by the discrete variable $\varepsilon_i(T)$, which is given by the autoregressive process³⁰, as:

$$\varepsilon_i(T + 1) = k\varepsilon_i(T) + \sigma\sqrt{1 - k^2} \frac{\varphi(T) + \beta\omega_i(T)}{\sqrt{1 + \beta^2}} \quad (2)$$

$$\beta = \sqrt{\frac{1 - |\rho|}{|\rho|}}$$

342 where T is the discrete time point (0, 1, 2 ... 1000), k is the autocorrelation coefficient, and ρ
343 is the species response correlation – the correlation between all pairs of specific response ε_i .
344 The terms $\varphi(T)$ and $\omega_i(T)$ are standard normal random components, where the former is
345 consistent for all species and the latter differs between species. Parameter β is a scaling factor
346 ensuring that noise variance remains independent of ρ . This method scales the noise time
347 series to its asymptotical variance σ_i^2 independently of noise autocorrelation^{30,61}. We
348 simulated a range of regimes of environmental stochasticity within a fully-crossed design
349 using k and ρ . k was set to -0.8, -0.4, 0, 0.4, and 0.8, reflecting ranges in colour from blue
350 through white to red, while ρ was set to 0.2, 0.5, and 0.8 (with 0 corresponding to no
351 correlation among species and 1 corresponding to perfect correlation). There were, therefore,
352 15 (*i.e.* 5×3) fully-crossed combinations of k and ρ . We arbitrarily set σ_i^2 to 0.05 for
353 simplicity. Changing the level of set σ_i^2 does not affect our conclusions about the general
354 effects of k and ρ on the response and predictability of ecological stability (results not shown
355 here). The unique combination of stochasticity features all led to different stochasticity
356 regimes determined by the random terms $\varphi(T)$ and $\omega_i(T)$. We produced 50 sets of $\varphi(T)$ and
357 $\omega_i(T)$, and applied them to each unique combination of stochasticity features to build 50
358 ‘replicated’ regimes of environmental stochasticity, which were then used for every model
359 community.

360 Most models comparing coloured environments with white noise assume implicitly that
361 the normality of the noise time series is retained as its temporal autocorrelation changes from
362 zero to either positive or negative values^{40,62}. However, Fowler and Ruokolainen⁶³ showed
363 that coloured series tend to deviate from the normal distribution when using common
364 approaches to generate time series of coloured environmental stochasticity, and this can

365 confound the effect of environmental colour on dynamical processes. Cohen *et al.*⁶⁴
366 developed 'spectral mimicry' approach, to transform a coloured environmental series that does
367 not follow a normal frequency distribution to a new series with a normal distribution yet
368 maintaining the original level of temporal autocorrelation. Briefly, spectral mimicry takes two
369 input series of equal length, X and Y , and reorders one series (Y) to generate a third series (Z)
370 that approximates the temporal characteristics (colour) of (X). (X) is a traditional coloured
371 series that was generated by the autoregressive process defined by Equations (1) & (2), and
372 (Y) is an independent random series drawn from a standard normal distribution (mean = 0,
373 standard deviation = 1). Only random series Y that failed to reject the null hypothesis of a
374 Jarque-Bera statistical test (*i.e.* that there is no evidence that data deviate from a normal
375 distribution; significance level $\alpha = 0.05$) were selected for further use. The elements
376 of X were ranked in increasing value, with their *order statistics* recorded from the original
377 series. Series Z was then generated from Y "by replacing each element of Y by the
378 corresponding *order statistic* of X "⁶⁴. This algorithm results in series Z having a spectral
379 exponent similar to that of X . For each environmental stochasticity time series generated
380 using the autoregressive process (equation 2), we used spectral mimicry to generate another
381 time series to avoid artefacts in the results known to be caused by traditional AR(1)
382 methods⁶³. Both the autoregressive method and spectral mimicry produced the desired
383 temporal autocorrelation and species response correlation (Supplementary Figs. 5 and 6). For
384 simplicity, we report only the results that used spectral mimicry to generate environmental
385 stochasticity, though the general features of our results are consistent with those from
386 autoregression. In summary, we produced $5(k) \times 3(\rho) \times 50(\text{realisations}) = 750$ stochasticity
387 regimes for each of our 1400 communities (100 communities \times 14 modules).

388

389 *Ecological stability*

390 We simulated species dynamics for all food-webs with the locally stable equilibrium as
391 the initial state value for every replicate stochasticity regime. In parallel, we also simulated
392 their dynamics with a 50% reduction in the equilibrium biomass of the species at the highest

393 trophic level in each food-web module as the initial state value under the same stochasticity
394 regime. The latter corresponded to the ‘perturbed’ treatment for each replicate stochasticity
395 regime. Coupling the simulations with and without initial perturbation adds ecological realism
396 compared to previous studies, which tend to investigate only one of them (but see⁶⁵).
397 Simulations of dynamics of both the ‘unperturbed’ and ‘perturbed’ community were run over
398 1000 time steps with a step length of 1. The time allowed almost all (> 99.9%) of the
399 simulated communities to recover fully (Supplementary Fig. 7). The simulations were
400 performed in *R* version 3.2.4⁶⁶ using the 'deSolve' library⁶⁷ with the solver 'lsoda'.

401 Because predators tend to be particularly important drivers of community dynamics
402 and stability^{7,31-33}, we examined the responses of our simulated communities to instantaneous
403 reductions in the densities of the apex predator in the system. However, we also explored
404 whether the effect of environmental stochasticity on stability and its uncertainty are sensitive
405 to the identity of the species receiving the pulse perturbation by perturbing each of the four
406 species of the diamond module in isolation (*i.e.* Module 2 in Supplementary Fig. 1). We
407 found that the general effect of environmental autocorrelation on the response and
408 predictability of the various dimensions of ecological stability we quantified is robust to the
409 identity of the consumer species receiving perturbations, but that this was not the case for the
410 basal species (Supplementary Fig. 8). Rather, the relatively high abundances and intrinsic
411 growth rates of the basal species enabled them to compensate rapidly for the initial reduction
412 in their population densities in perturbed communities. This resulted in the Euclidean distance
413 of the perturbed community decreasing monotonically from its equilibrium immediately
414 following the perturbation and, thus, the maximum distance between perturbed and
415 unperturbed communities occurring at the point of perturbation itself. Because of this, the
416 extent of community change caused by the perturbation was unaffected by the temporal
417 autocorrelation of environmental stochasticity when the basal species was perturbed in
418 isolation (Supplementary Fig. 8). Given this, our results may not extend to situations where a
419 direct and isolated pulse perturbation is conducted on a species with an extremely rapid

420 response and where there is barely time for short-term environmental structure to have any
421 obvious impact.

422 The recovery time for each food-web simulation was quantified as the time when the
423 difference between the ‘unperturbed’ and ‘perturbed’ community dynamics reduced to a
424 critical level (Fig. 1b). This corresponded to the first timestep when the difference between
425 the densities of all species in the perturbed and unperturbed communities was less than 0.01
426 and this difference was maintained for at least 50 timesteps thereafter to ensure convergence
427 had been achieved. The maximum Euclidean distance between perturbed and unperturbed
428 communities, which we measured at each simulation step, was used to measure resistance
429 (Fig. 1c). Increases in Euclidian distance correspond to reductions in resistance, and *vice*
430 *versa*²². We quantified variability as the standard deviation of the total density of the
431 unperturbed community during the simulation time window divided by its mean (Fig. 1d). As
432 variability is a function of time, we also explored how the duration of the time window over
433 which it was quantified affects our measure of variability and its uncertainty. We therefore
434 measured variability over both the entire time series of the simulations and during only the
435 recovery period (*i.e.* ‘transient’ variability). We found that both variability measures
436 responded similarly to the temporal autocorrelation of environmental noise, though the
437 uncertainty associated with transient variability was markedly higher than for when variability
438 was measured over the entire time series (Supplementary Fig. 2). We report only the results of
439 variability measured over the entire time-series of the simulations in the manuscript.

440

441 *Random forest regression*

442 We examined the capacity of environmental stochasticity and a range of community
443 and module characteristics (see Fig. 5 for full list of explanatory variables used in the models)
444 to explain the responses of each of our three focal stability dimensions using random forest
445 regression at two analytical scales. The first includes the data from across all of the individual
446 replicate ($n = 50$) stochasticity regimes for each distinct community, and thus incorporates
447 variation in responses of food-webs to distinct runs of environmental stochasticity (*i.e.* the

448 specific temporal responses of communities) described by autocorrelation and species
449 response correlation, while the second omits the variation across these replicate stochasticity
450 regimes to focus only on the mean stability response of each community for each stochasticity
451 treatment combination, indicating the general response pattern at the level of each food-web.
452 The random forest algorithm converges on an optimal solution from individual solutions of
453 multiple trees (500 regression trees in this case) using bootstrapping and is non-parametric,
454 not subject to distributional assumptions, compatible with categorical, ordinal, and continuous
455 data simultaneously, invariant to outliers and monotonic transformations of variables, and
456 capable of handling high-dimensional data and identifying and incorporating complex
457 variable interactions^{68,69}. Random forest regression was therefore appropriate for analysis of
458 our multiple-layer dataset given the skewed distribution and nonlinear responses of many of
459 our stability components (*e.g.* Supplementary. Fig. 7) and the need to include both continuous
460 and categorical variables as predictors. The importance of each predictor in the random forest
461 is computed from permuting out-of-bag (OOB) data⁷⁰. For each tree, the prediction (mean-
462 squared) error on the OOB portion of the data was recorded. The same was then done after
463 permuting each of the predictors. The differences between the two are then averaged across
464 all trees, and normalized by the standard deviation of the differences. The random forest
465 regression model was conducted in *R* version 3.2.4⁶⁶ using the 'ranger' library⁷¹.

466

467 **Data availability** All core data including the constructed communities, time series of
468 environmental stochasticity, and ecological stabilities, and the R codes for generating the
469 results and figures of this paper will be uploaded to Dryad repository and open to the public.

470

471 **References**

- 472 1 Bellard, C., Bertelsmeier, C., Leadley, P., Thuiller, W. & Courchamp, F. Impacts of
473 climate change on the future of biodiversity. *Ecol. Lett.* **15**, 365-377 (2012).
474 2 Blois, J. L., Zarnetske, P. L., Fitzpatrick, M. C. & Finnegan, S. Climate change and
475 the past, present, and future of biotic interactions. *Science* **341**, 499-504 (2013).
476 3 Davis, A. J., Jenkinson, L. S., Lawton, J. H., Shorrocks, B. & Wood, S. Making
477 mistakes when predicting shifts in species range in response to global warming.
478 *Nature* **391**, 783-786 (1998).

479 4 Oliver, T. H. *et al.* Biodiversity and resilience of ecosystem functions. *Trends Ecol. Evolut.* **30**, 673-684 (2015).

480

481 5 Petchey, O. L. *et al.* The ecological forecast horizon, and examples of its uses and
482 determinants. *Ecol. Lett.* **18**, 597-611 (2015).

483 6 Urban, M. C. *et al.* Improving the forecast for biodiversity under climate change.
484 *Science* **353**, aad8466 (2016).

485 7 Donohue, I. *et al.* Loss of predator species, not intermediate consumers, triggers rapid
486 and dramatic extinction cascades. *Glob. Change Biol.* **23**, 2962-2972 (2017).

487 8 Thompson, R. M., Beardall, J., Beringer, J., Grace, M. & Sardina, P. Means and
488 extremes: building variability into community-level climate change experiments.
489 *Ecol. Lett.* **16**, 799-806 (2013).

490 9 Donohue, I. *et al.* Navigating the complexity of ecological stability. *Ecol. Lett.* **19**,
491 1172-1185 (2016).

492 10 Vellend, M. *The theory of ecological communities.* (Princeton University Press,
493 2016).

494 11 Boettiger, C. From noise to knowledge: how randomness generates novel phenomena
495 and reveals information. *Ecol. Lett.* **21**, 1255-1267 (2018).

496 12 Halley, J. M. Ecology, evolution and 1/f-noise. *Trends Ecol. Evolut.* **11**, 33-37
497 (1996).

498 13 Ruokolainen, L., Linden, A., Kaitala, V. & Fowler, M. S. Ecological and evolutionary
499 dynamics under coloured environmental variation. *Trends Ecol. Evolut.* **24**, 555-563
500 (2009).

501 14 Vasseur, D. A. & Yodzis, P. The color of environmental noise. *Ecology* **85**, 1146-
502 1152 (2004).

503 15 Easterling, D. R. *et al.* Climate extremes: observations, modeling, and impacts.
504 *Science* **289**, 2068-2074 (2000).

505 16 Jentsch, A., Kreyling, J., Boettcher-Treschkow, J. & Beierkuhnlein, C. Beyond
506 gradual warming: extreme weather events alter flower phenology of European
507 grassland and heath species. *Glob. Change Biol.* **15**, 837-849 (2009).

508 17 Kayler, Z. E. *et al.* Experiments to confront the environmental extremes of climate
509 change. *Front. Ecol. Environ.* **13**, 219-225 (2015).

510 18 Kuparinen, A., Keith, D. M. & Hutchings, J. A. Increased environmentally driven
511 recruitment variability decreases resilience to fishing and increases uncertainty of
512 recovery. *ICES J. Mar. Sci.* **71**, 1507-1514 (2014).

513 19 Crone, E. E. Contrasting effects of spatial heterogeneity and environmental
514 stochasticity on population dynamics of a perennial wildflower. *J. Ecol.* **104**, 281-291
515 (2016).

516 20 Fowler, M. S. & Ruokolainen, L. Colonization, covariance and colour:
517 Environmental and ecological drivers of diversity-stability relationships. *J. Theor.*
518 *Biol.* **324**, 32-41 (2013).

519 21 Ruokolainen, L., Ranta, E., Kaitala, V. & Fowler, M. S. Community stability under
520 different correlation structures of species' environmental responses. *J. Theor. Biol.*
521 **261**, 379-387 (2009).

522 22 Donohue, I. *et al.* On the dimensionality of ecological stability. *Ecol. Lett.* **16**, 421-
523 429 (2013).

524 23 Pimm, S. L. The complexity and stability of ecosystems. *Nature* **307**, 321-326 (1984).

525 24 Ives, A. R. & Carpenter, S. R. Stability and diversity of ecosystems. *Science* **317**, 58-
526 62 (2007).

527 25 May, R. M. *Stability and complexity in model ecosystems.* (Princeton University
528 Press, 1973).

529 26 Sabo, J. L. & Post, D. M. Quantifying periodic, stochastic, and catastrophic
530 environmental variation. *Ecol. Monogr.* **78**, 19-40 (2008).

531 27 Pimm, S. L. & Lawton, J. H. Number of trophic levels in ecological communities.
532 *Nature* **268**, 329-331 (1977).

- 533 28 Pimm, S. L. & Lawton, J. H. On feeding on more than one trophic level. *Nature* **275**,
534 542-544 (1978).
- 535 29 Petchey, O. L., Eklof, A., Borrvall, C. & Ebenman, B. Trophically unique species are
536 vulnerable to cascading extinction. *Am. Nat.* **171**, 568-579 (2008).
- 537 30 Ruokolainen, L. & Fowler, M. S. Community extinction patterns in coloured
538 environments. *Proc. Royal Soc. B* **275**, 1775-1783 (2008).
- 539 31 Estes, J. A. *et al.* Trophic downgrading of planet Earth. *science* **333**, 301-306 (2011).
- 540 32 O'Connor, N. E., Emmerson, M. C., Crowe, T. P. & Donohue, I. Distinguishing
541 between direct and indirect effects of predators in complex ecosystems. *J. Anim.*
542 *Ecol.* **82**, 438-448 (2013).
- 543 33 White, L., Donohue, I., Emmerson, M. C. & O'Connor, N. E. Combined effects of
544 warming and nutrients on marine communities are moderated by predators and vary
545 across functional groups. *Glob. Change Biol.*, doi:10.1111/gcb.14456 (2018).
- 546 34 Bascompte, J. & Melian, C. J. Simple trophic modules for complex food webs.
547 *Ecology* **86**, 2868-2873 (2005).
- 548 35 Kondoh, M. Building trophic modules into a persistent food web. *Proc. Natl. Acad.*
549 *Sci. U.S.A* **105**, 16631-16635 (2008).
- 550 36 Milo, R. *et al.* Network motifs: simple building blocks of complex networks. *Science*
551 **298**, 824-827 (2002).
- 552 37 Clark, J. S. Uncertainty and variability in demography and population growth: A
553 hierarchical approach. *Ecology* **84**, 1370-1381 (2003).
- 554 38 Clark, J. S. Individuals and the variation needed for high species diversity in forest
555 trees. *Science* **327**, 1129-1132 (2010).
- 556 39 Laakso, J., Kaitala, V. & Ranta, E. Non-linear biological responses to environmental
557 noise affect population extinction risk. *Oikos* **104**, 142-148 (2004).
- 558 40 Ripa, J. & Heino, M. Linear analysis solves two puzzles in population dynamics: the
559 route to extinction and extinction in coloured environments. *Ecol. Lett.* **2**, 219-222
560 (1999).
- 561 41 Loreau, M. & de Mazancourt, C. Biodiversity and ecosystem stability: a synthesis of
562 underlying mechanisms. *Ecol. Lett.* **16**, 106-115 (2013).
- 563 42 Tilman, D. Biodiversity: Population versus ecosystem stability. *Ecology* **77**, 350-363
564 (1996).
- 565 43 Wang, S. P. & Loreau, M. Biodiversity and ecosystem stability across scales in
566 metacommunities. *Ecol. Lett.* **19**, 510-518 (2016).
- 567 44 Ives, A. R., Gross, K. & Klug, J. L. Stability and variability in competitive
568 communities. *Science* **286**, 542-544 (1999).
- 569 45 Kalinkat, G. *et al.* Body masses, functional responses and predator-prey stability.
570 *Ecol. Lett.* **16**, 1126-1134 (2013).
- 571 46 Kaneryd, L. *et al.* Species-rich ecosystems are vulnerable to cascading extinctions in
572 an increasingly variable world. *Ecol. Evol.* **2**, 858-874 (2012).
- 573 47 Berlow, E. L. *et al.* Simple prediction of interaction strengths in complex food webs.
574 *Proc. Natl. Acad. Sci. U.S.A* **106**, 187-191 (2009).
- 575 48 van der Bolt, B., van Nes, E. H., Bathiany, S., Vollebregt, M. E. & Scheffer, M.
576 Climate reddening increases the chance of critical transitions. *Nat. Clim. Chang.* **8**,
577 478-484 (2018).
- 578 49 Scheffer, M. *et al.* Early-warning signals for critical transitions. *Nature* **461**, 53
579 (2009).
- 580 50 Greenman, J. V. & Benton, T. G. The amplification of environmental noise in
581 population models: causes and consequences. *Am. Nat.* **161**, 225-239 (2003).
- 582 51 Murdoch, W. M., Briggs, C. J. & Nisbet, R. M. *Consumer-resource dynamics*.
583 (Princeton University Press, 2003).
- 584 52 Mayfield, M. M. & Stouffer, D. B. Higher-order interactions capture unexplained
585 complexity in diverse communities. *Nat. Ecol. Evol.* **1**, 0062 (2017).

586 53 Cohen, J. E., Jonsson, T. & Carpenter, S. R. Ecological community description using
587 the food web, species abundance, and body size. *Proc. Natl. Acad. Sci. U.S.A* **100**,
588 1781-1786 (2003).

589 54 Brown, J. H., Gillooly, J. F., Allen, A. P., Savage, V. M. & West, G. B. Toward a
590 metabolic theory of ecology. *Ecology* **85**, 1771-1789 (2004).

591 55 Healy, K. *et al.* Ecology and mode-of-life explain lifespan variation in birds and
592 mammals. *Proc. Royal Soc. B* **281**, 20140298 (2014).

593 56 Paine, R. T. Food-web analysis through field measurement of per-capita interaction
594 strength. *Nature* **355**, 73-75 (1992).

595 57 Wootton, J. T. & Emmerson, M. Measurement of interaction strength in nature. *Annu.*
596 *Rev. Ecol. Evol. Syst.* **36**, 419-444 (2005).

597 58 Emmerson, M. & Yearsley, J. M. Weak interactions, omnivory and emergent food-
598 web properties. *Proc. Royal Soc. B* **271**, 397-405 (2004).

599 59 Gilpin, M. E. Stability of feasible predator-prey systems. *Nature* **254**, 137-139
600 (1975).

601 60 Jansen, V. A. A. & Kokkoris, G. D. Complexity and stability revisited. *Ecol. Lett.* **6**,
602 498-502 (2003).

603 61 Heino, M., Ripa, J. & Kaitala, V. Extinction risk under coloured environmental noise.
604 *Ecography* **23**, 177-184 (2000).

605 62 Greenman, J. V. & Benton, T. G. The impact of environmental fluctuations on
606 structured discrete time population models: Resonance, synchrony and threshold
607 behaviour. *Theor. Popul. Biol.* **68**, 217-235 (2005).

608 63 Fowler, M. S. & Ruokolainen, L. Confounding environmental colour and distribution
609 shape leads to underestimation of population extinction risk. *Plos One* **8** (2013).

610 64 Cohen, J. E., Newman, C. M., Cohen, A. E., Petchey, O. L. & Gonzalez, A. Spectral
611 mimicry: A method of synthesizing matching time series with different Fourier
612 spectra. *Circ. Syst. Signal PR* **18**, 431-442 (1999).

613 65 Ruokolainen, L., Fowler, M. S. & Ranta, E. Extinctions in competitive communities
614 forced by coloured environmental variation. *Oikos* **116**, 439-448 (2007).

615 66 R Core Team. R: A language and environment for statistical computing. R
616 Foundation for Statistical Computing, Vienna, Austria. URL [https://http://www.R-](https://http://www.R-project.org/)
617 [project.org/](https://http://www.R-project.org/). (2016).

618 67 Soetaert, K., Petzoldt, T. & Setzer, R. W. Solving differential equations in R: package
619 deSolve. *J. Stat. Softw.* **33**, 1-25 (2010).

620 68 Evans, J. S., Murphy, M. A., Holden, Z. A. & Cushman, S. A. in *Predictive species*
621 *and habitat modeling in landscape ecology* (eds C. A. Drew, Y. Wiersma, & F.
622 Huettmann) 139-159 (Springer, 2011).

623 69 Shi, T. & Horvath, S. Unsupervised learning with random forest predictors. *J.*
624 *Comput. Graph. Stat.* **15**, 118-138 (2006).

625 70 Liaw, A. & Wiener, M. Classification and Regression by randomForest. . *R News* **2**,
626 18-22 (2002).

627 71 Wright, M. N. & Ziegler, A. ranger: A Fast Implementation of Random Forests for
628 High Dimensional Data in C++ and R. *J. Stat. Softw.* **77**, 1-17 (2017).

629

630

631 **Fig. 1 | Quantification of ecological stability dimensionms. a.** A typical example of
632 community dynamics. **b.** The species density difference between perturbed and the equivalent
633 unperturbed communities at each simulation timestep. Recovery time was quantified as the
634 moment when the species density difference is smaller than 0.01 for all species (indicated for
635 each species by +; see *Methods*). **c.** The extent of change of the community (our measure of
636 resistance) was quantified as the largest Euclidean distance between perturbed and their
637 equivalent unperturbed community. **d.** Variability was quantified as the standard deviation of
638 the total density of the unperturbed community divided by its mean value.

639

640 **Fig. 2 | Stability responses of a single food-chain community to replicate regimes of**
641 **environmental stochasticity along a gradient in temporal autocorrelation. a.** Changes in
642 recovery time, the extent of change in community structure and variability in a single example
643 food-chain community along a gradient in temporal autocorrelation. Every point at each level
644 of autocorrelation represents the stability response of one of 50 noise replicates (distinct runs
645 of stochastic noise described by identical autocorrelation; see *Methods*) for the community.
646 All responses are inversely related to stability (*i.e.* stability decreases from the bottom to the
647 top of the y-axis in every case). The solid line corresponds to the mean response for the
648 community across noise replicates and, therefore, indicates the general response of each
649 stability component to the temporal autocorrelation of environmental noise. **b.** Uncertainty in
650 stability responses of the community to the temporal autocorrelation of environmental noise.
651 This was quantified as the coefficient of variation (standard deviation divided by the mean)
652 across the noise replicates. High uncertainty corresponds to low predictability of ecological
653 stability. For this illustrative example, the correlation of species responses to environmental
654 fluctuations was set to 0.2.

655

656 **Fig. 3 | General stability responses to changes in environmental autocorrelation across a**
657 **diverse range of food-web modules. a.** General stability responses and **b.** uncertainty of
658 those responses to changes in environmental autocorrelation. Individual lines in a. and b.

659 correspond, respectively, to the mean and coefficient of variation in the response across 50
660 noise replicates for each of the 100 communities of each module structure. All responses in a.
661 are inversely related to stability (*i.e.* stability decreases from the bottom to the top of the y-
662 axis in every case). For this illustrative example, the correlation of species responses to
663 environmental fluctuations was set to 0.2.

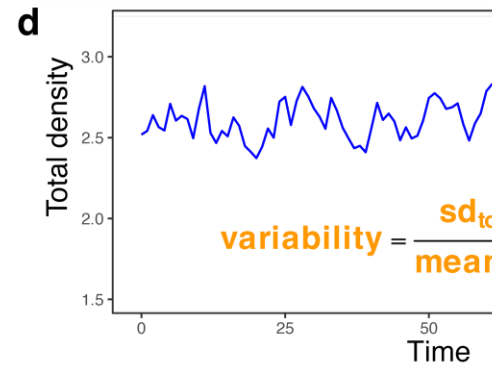
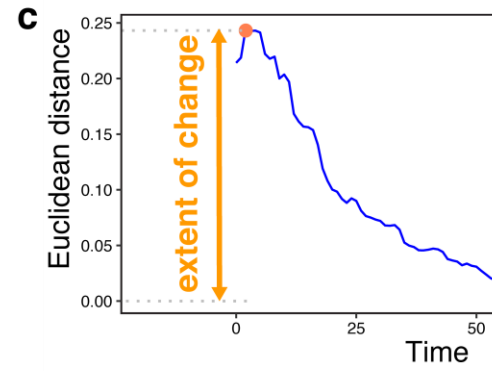
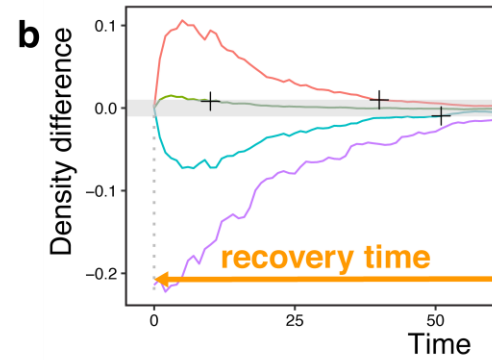
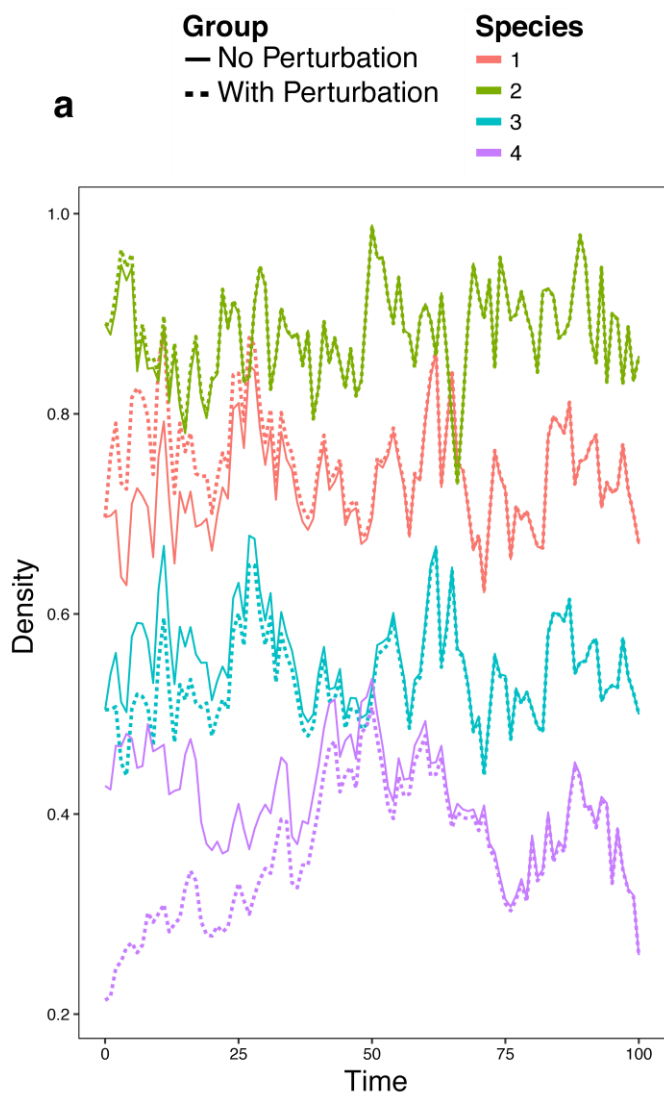
664

665 **Fig. 4 | General stability responses to changes in the correlation of species responses to**
666 **environmental fluctuations across a diverse range of food-web modules. a.** General
667 stability responses and **b.** uncertainty of those responses to changes in species environmental
668 response correlations. Individual lines in a. and b. correspond, respectively, to the mean and
669 coefficient of variation in the response across 50 noise replicates for each of the 100
670 communities of each module structure. All responses in a. are inversely related to stability
671 (*i.e.* stability decreases from the bottom to the top of the y-axis in every case). For this
672 illustrative example, the temporal autocorrelation of environmental noise was set to 0.8.

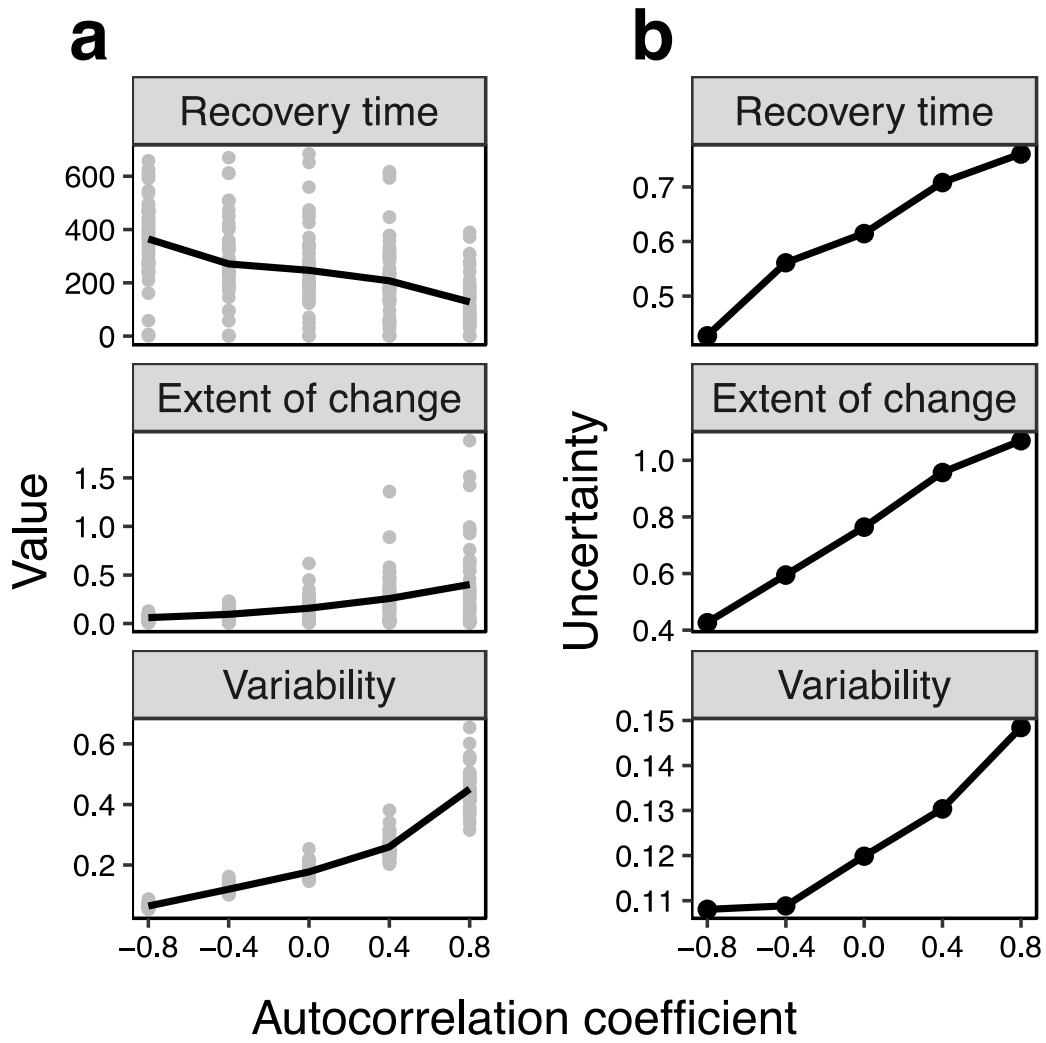
673

674 **Fig. 5 | The determinants of ecological stability in stochastic environments. a.**
675 Explanatory power (pseudo- R^2 of random forest regression models) of environmental
676 stochasticity and community and module characteristics in determining both the general
677 response pattern (the mean stability response across noise replicates, $n = 21,000$) and the
678 specific temporal response (*i.e.* incorporating variation in responses of food-webs to distinct
679 runs of stochastic noise described by identical autocorrelation, $n = 1,050,000$) of stability
680 components to environmental autocorrelation. **b.** Relative importance of individual
681 determinants of stability, calculated as the importance value of each explanatory variable in
682 random forest regression models divided by the sum of the importance of all variables. The
683 following variables were included as determinants in the model: the autocorrelation
684 coefficient of environmental stochasticity (autocorrelation), the correlation of species
685 responses to environmental noise (correlation.species), the maximum real part of the
686 eigenvalue of the community matrix (max.real.eigen.J), the maximum equilibrium species

687 density (max.Neq), the minimum equilibrium species density (min.Neq), the slowest
688 growth/decay rate of the community (min.R), the mean value of the upper triangular
689 (mean.upper.tri.J), lower triangular (mean.lower.tri.J) and diagonal (mean.diag.J) entries of
690 the community matrix, the mean value of the upper triangular (mean.upper.tri.A), lower
691 triangular (mean.lower.tri.A) and diagonal (mean.diag.A) entries of the interaction coefficient
692 matrix, the number of trophic levels (n.trophic.levels), basal species (n.basal.species),
693 omnivorous species (n.omnivorous.species) and omnivorous links (n.omnivorous.links), food-
694 web connectance (connectance), and the presence of competitive links between basal species
695 (competition).

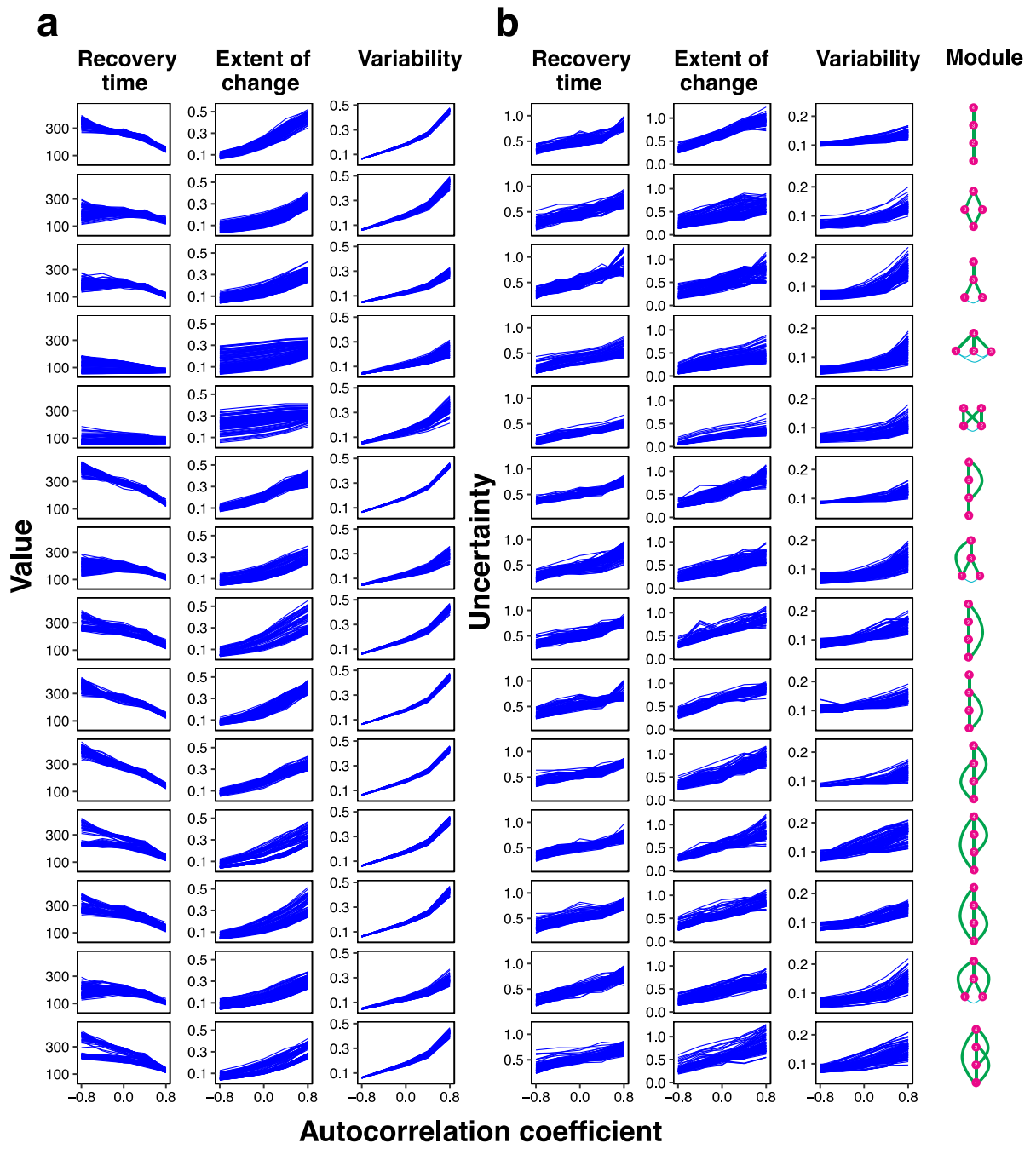


697
698
699



700
701
702

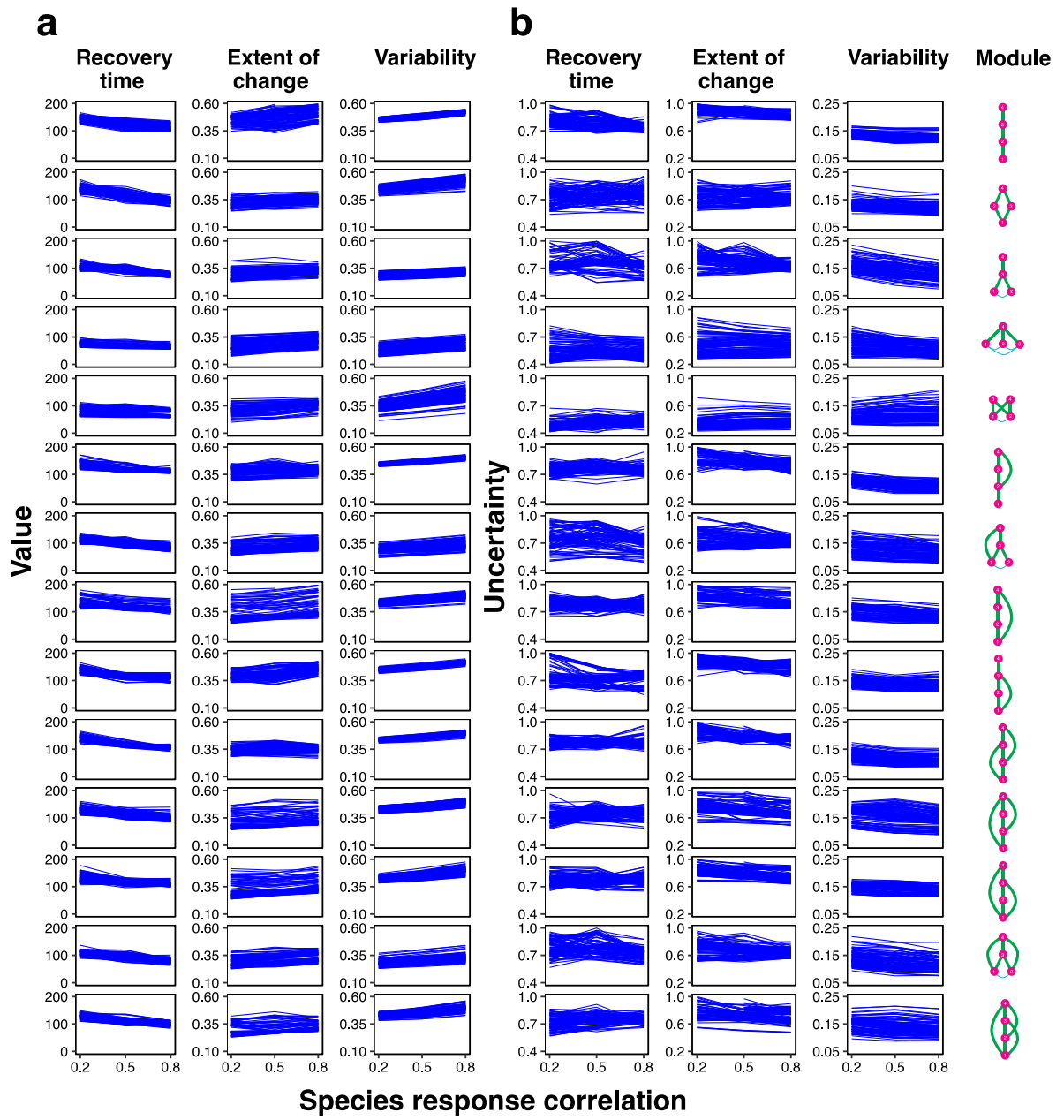
Yang et al. Fig. 2



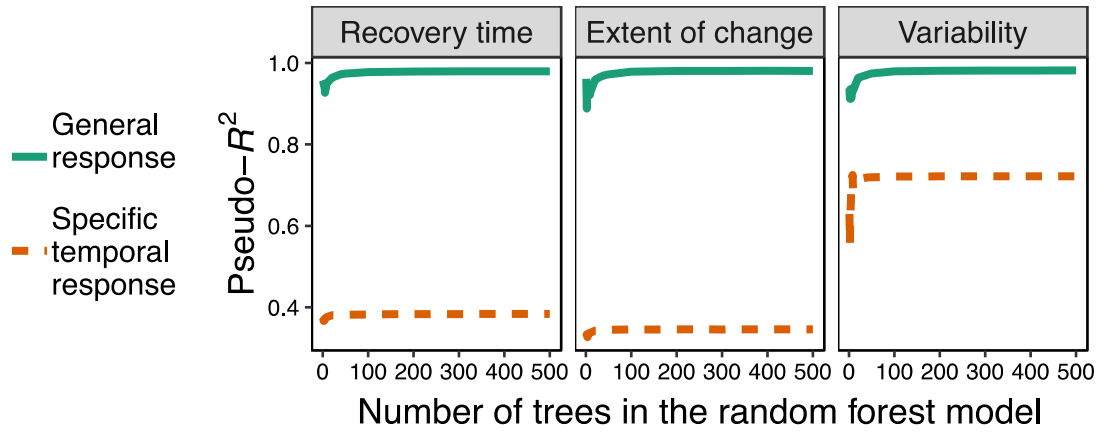
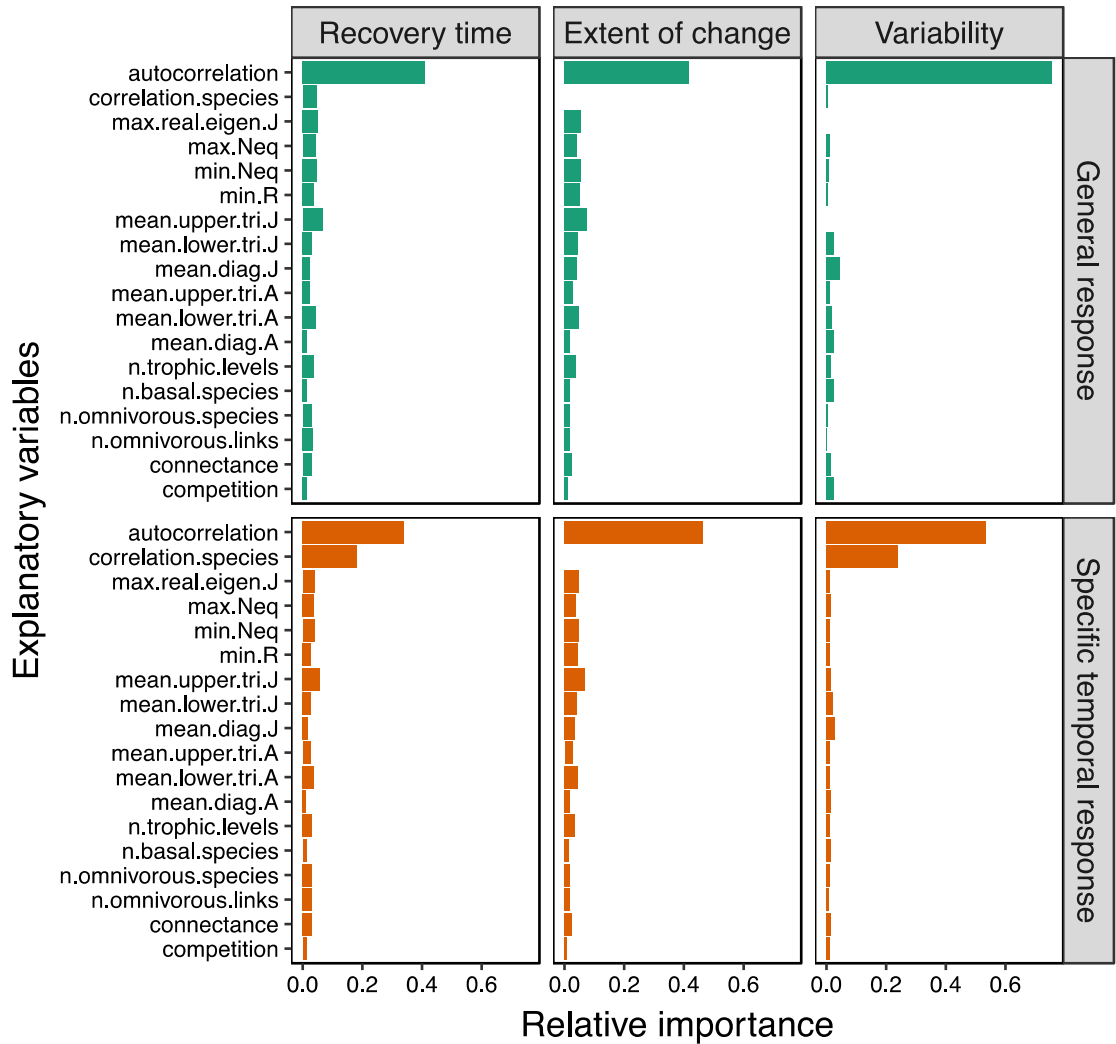
703

704

705



Yang et al. Fig. 4

a**b**

Yang et al. Fig. 5

The predictability of ecological stability in a noisy world

QIANG YANG^{1,2}, MIKE S. FOWLER³, ANDREW L. JACKSON¹, IAN DONOHUE¹

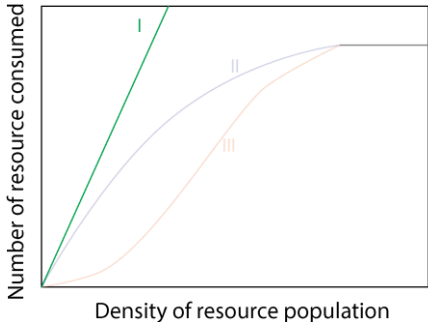
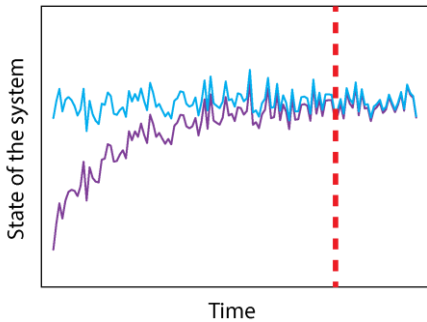
¹*Department of Zoology, School of Natural Sciences, Trinity College Dublin, Ireland*

²*Department of Biology, University of Konstanz, Konstanz, Germany*

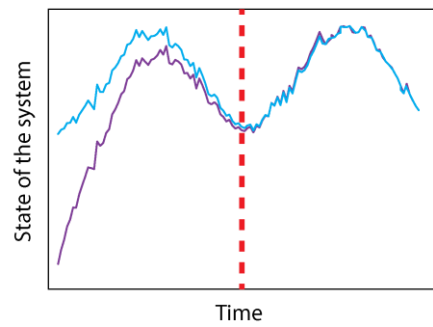
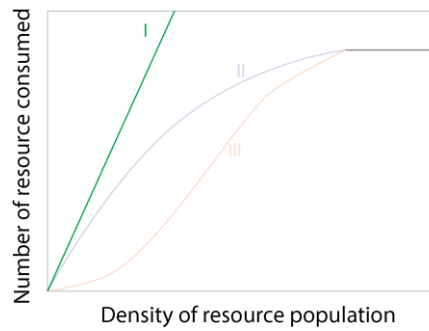
³*Department of Biosciences, Swansea University, Wales, UK*

Supplementary Material

Supplementary Table 1 | Influence of consumer functional response patterns on different components of ecological systems in a species consumer-resource system as an example. For simplicity, we assume the population density of the consumer is constant, so that the relationship between the density of the consumer and the resource can also be represented by the relationship between the density of the resource and the number of resource consumed. We consider the following four scenarios, where we compare the stability of the consumer-resource system under different functional response patterns and autocorrelation. **a.** The system follows the Type I functional response pattern. **b.** The system follows the Type II pattern, and the slope at equilibrium (indicated by the black point) is smaller than that at the perturbation point (indicated by the black point). **c.** The system also follows the Type III pattern, but the slope at the equilibrium is larger than that at the perturbation point.

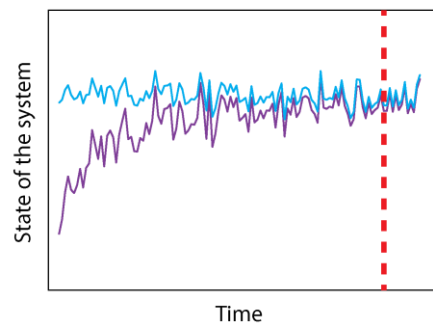
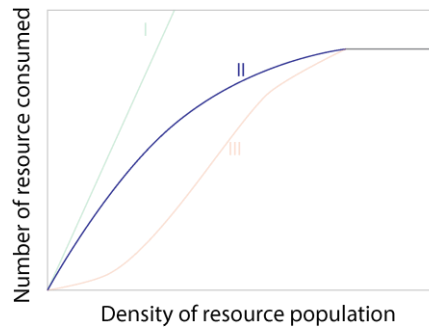
Autocorrelation of environmental stochasticity	Type of functional response	Response of the systems (— with perturbation, — without perturbation with regard to the color of the environmental stochasticity; dashed line represents the moment of recovery).	
a. Negative/zero autocorrelation			<p>Under negative autocorrelation (or zero autocorrelation, i.e., white noise), the mean state of the system is good environmental conditions and runs of poor environmental conditions can cancel each other out. So the system returns to equilibrium both the system with and without perturbation and the trajectory of the system without environmental stochasticity.</p>

Positive autocorrelation



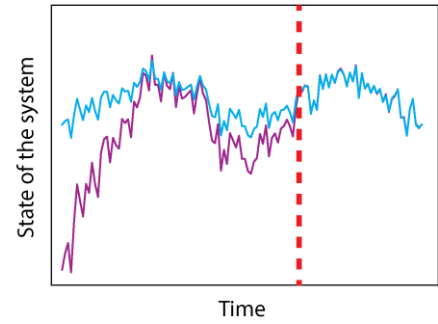
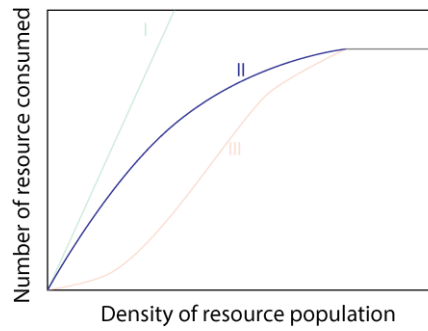
Under positive autocorrelation (red noise), the extreme environmental conditions caused by positive autocorrelation can cancel the effect of a perturbation. As a result, undercompensating populations are able to persist in the face of environmental fluctuations. Longer runs of favorable conditions are followed by longer runs of unfavorable conditions (high total biomass).

b. Negative/zero autocorrelation



The dynamics of a system with perturbations are similar with those of a system without perturbations. The system with negative/zero autocorrelation converges with the system without perturbations because the slow functional response of the perturbation is less than that at the equilibrium. Therefore, the consumer changes

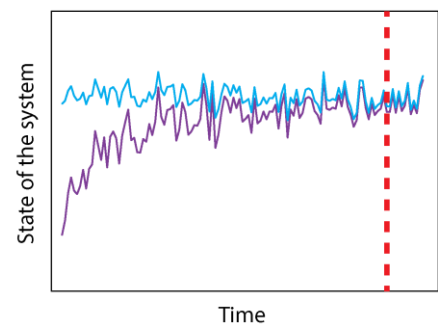
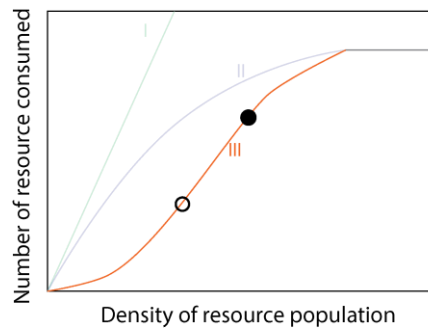
Positive autocorrelation



the variability of environmental conditions is larger at the perturbation point.

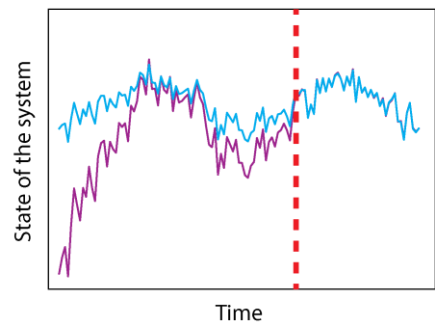
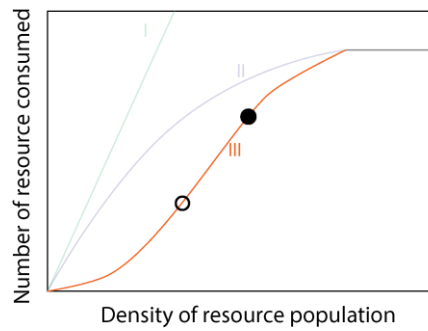
The dynamics of the system with perturbations are similar with those of a system without perturbations (*positive autocorrelation*). However, as the perturbation comes, the variability of the system with perturbations decreases.

c. Negative/zero autocorrelation



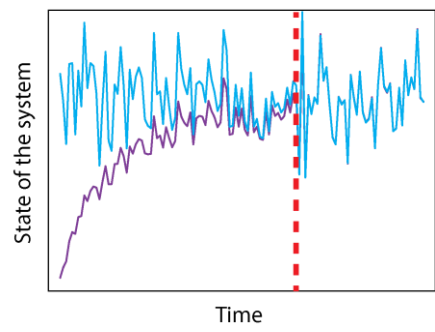
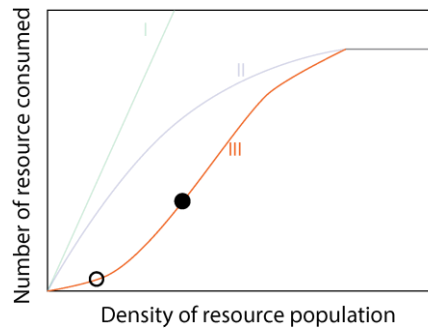
Similar with the case of *negative/zero autocorrelation*.

Positive autocorrelation



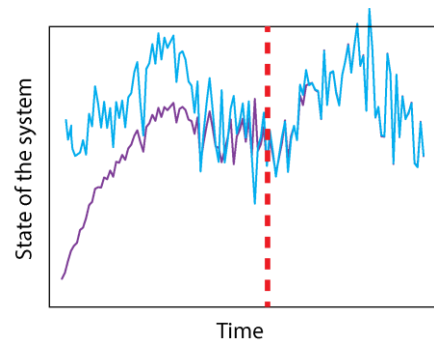
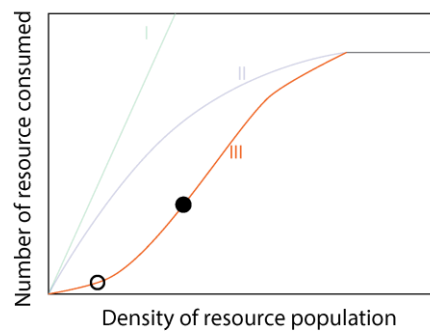
Similar to that autocorrelation

d. Negative/zero autocorrelation



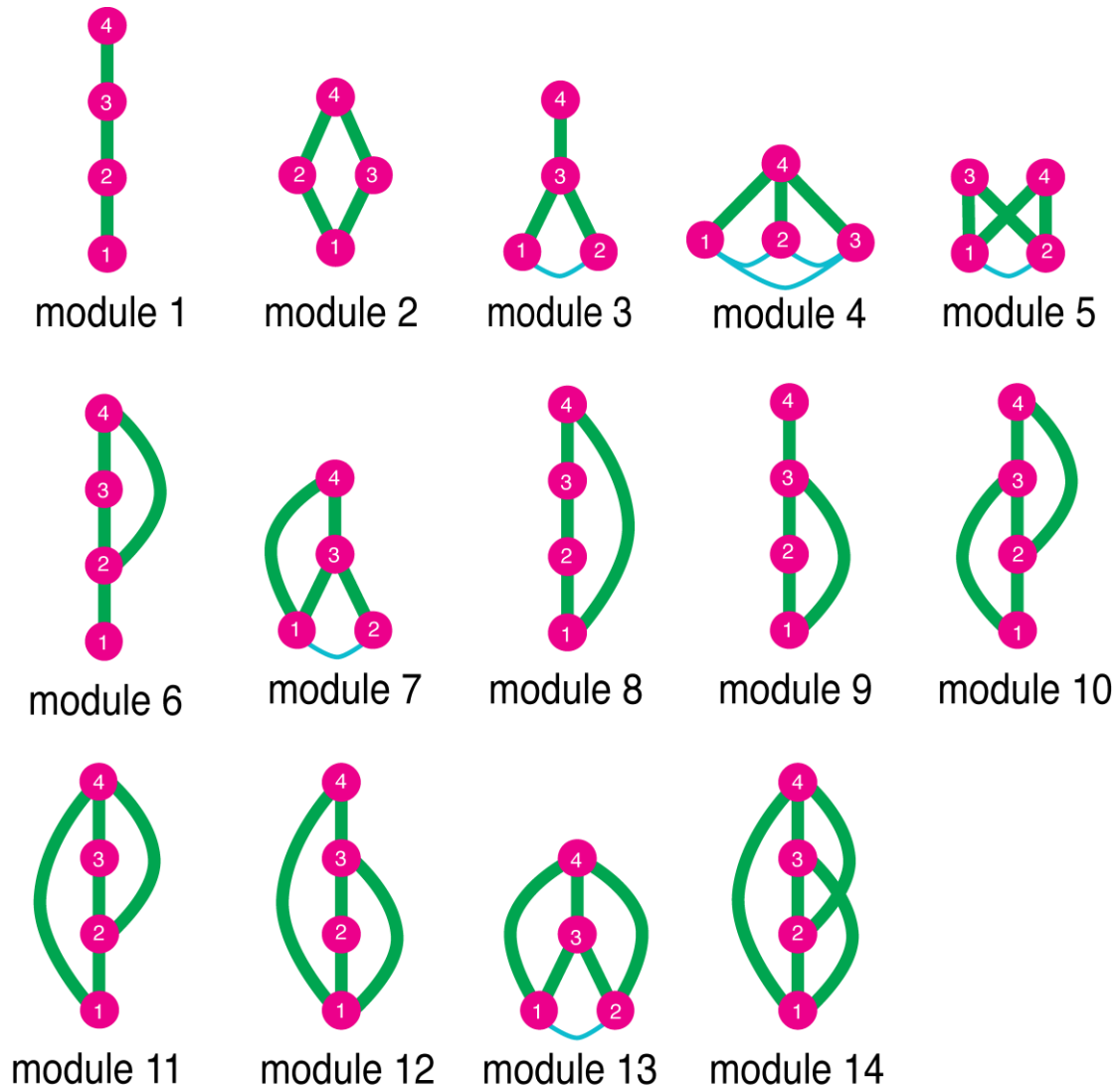
The dynamics with perturbation system without are similar with (negative/zero autocorrelation) the system with converges with without perturbation fluctuation increase because the slow functional response the perturbation smaller than the equilibrium. The biomass of the changes slower variability caused environmental

Positive autocorrelation

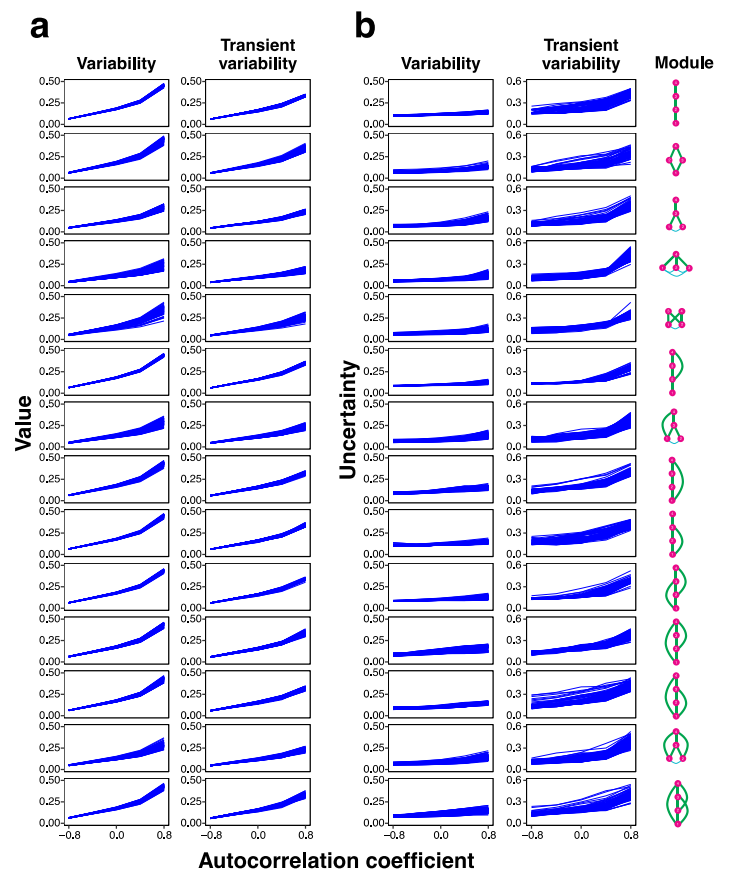


smaller at the p
point.

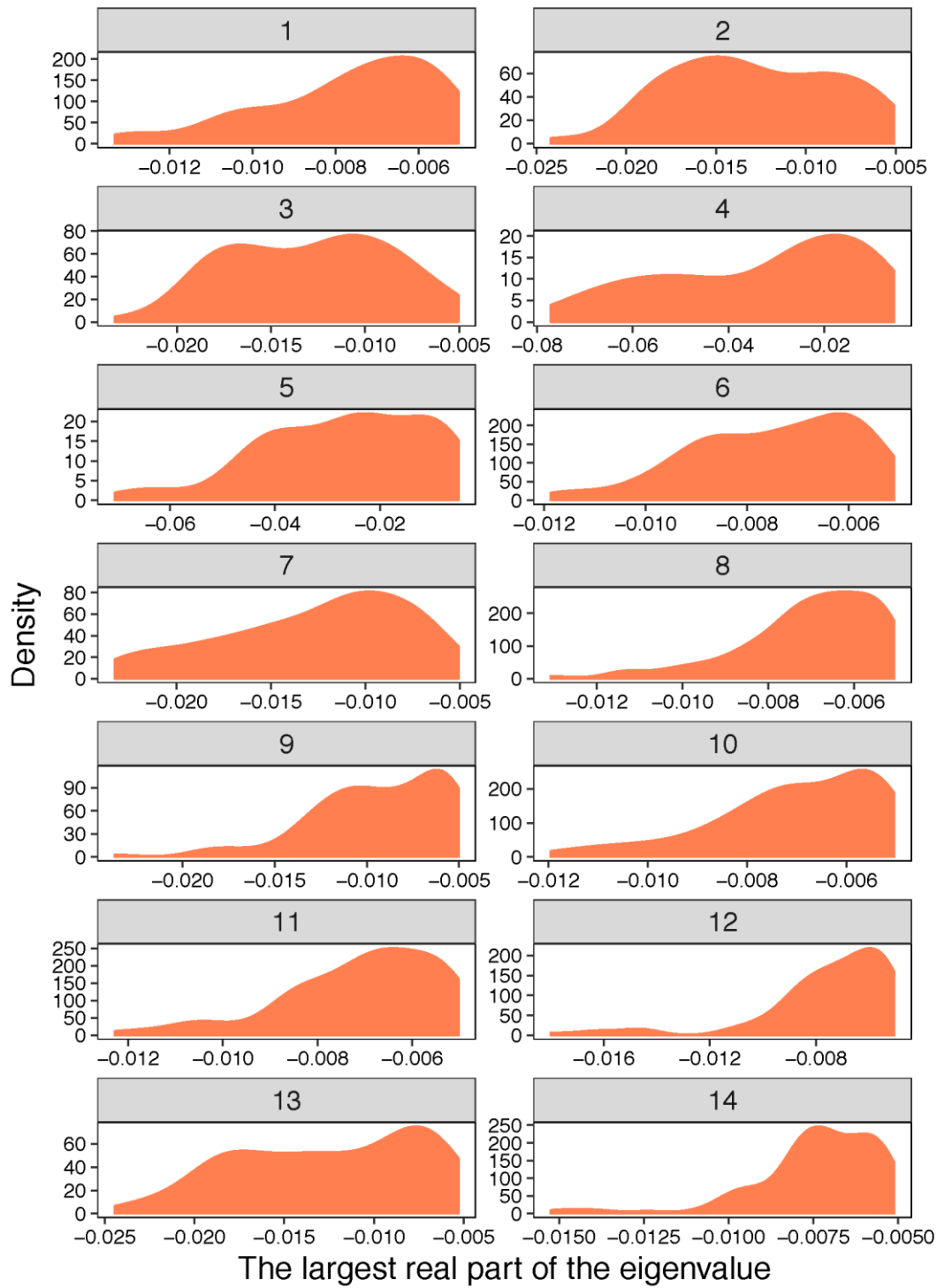
The dynamics
with perturbati
system without
are similar with
(positive autocorrelation)
However, as the
perturbation co
the system with
perturbation, the
increases.



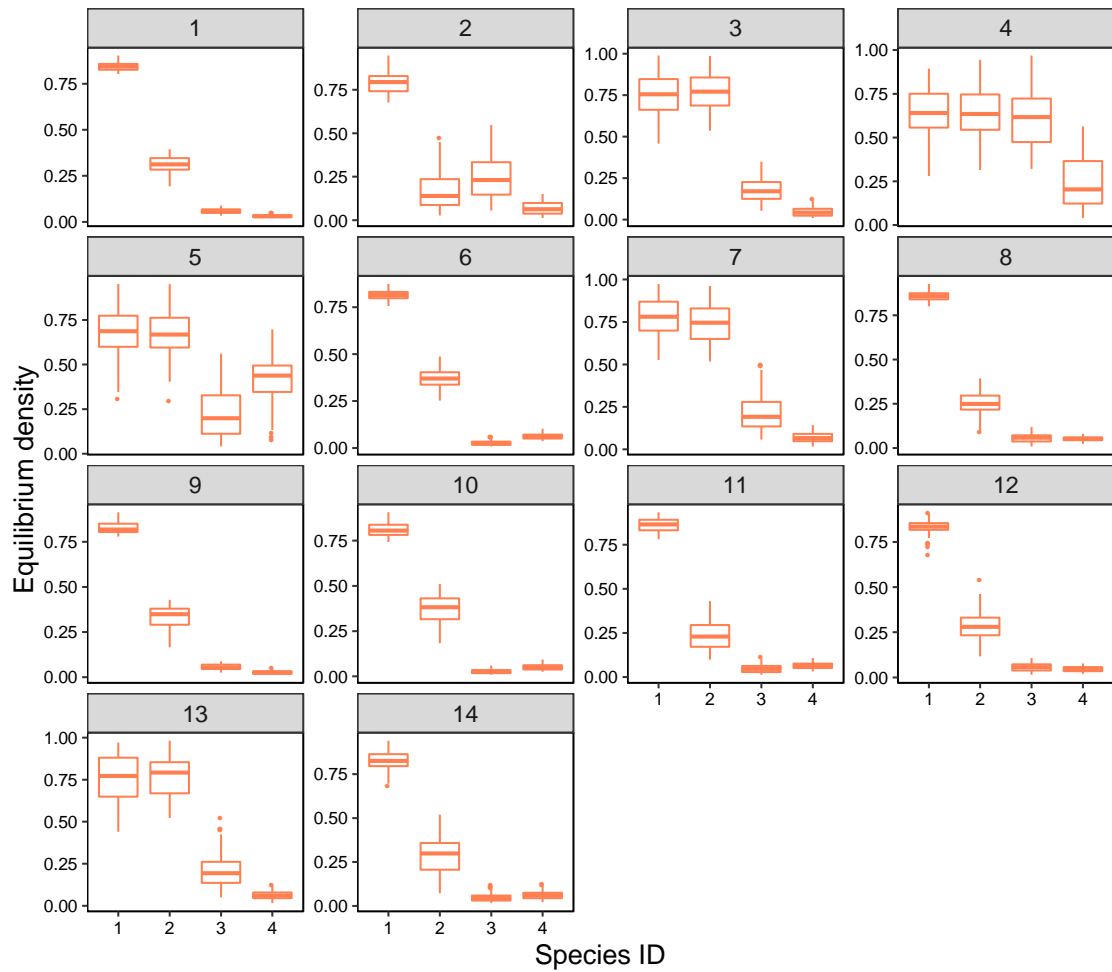
Supplementary Fig. 1 | Food-web modules used in our study. Pink points represent different species, with lower points as the resource and the upper points as consumers. Green lines indicate consumer-resource interactions. Cyan lines represent the competition between basal species.



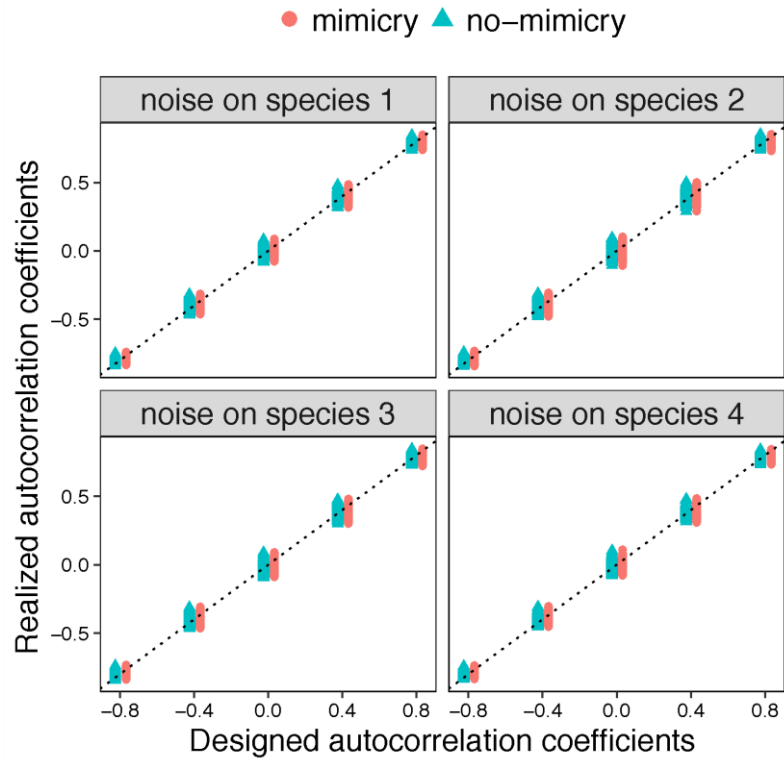
Supplementary Fig. 2 | Responses of variability measured across different time windows (*i.e.* long-term variability *Methods*) to changes in environmental autocorrelation across a diverse range of food-web modules. **a. General sta those responses to changes in environmental autocorrelation. Each line corresponds to the mean response across 50 noi communities of each module structure. All responses in a. are inversely related to stability (*i.e.* stability decreases from every case). For this illustrative example, the correlation of species responses to environmental fluctuations was set to 0**



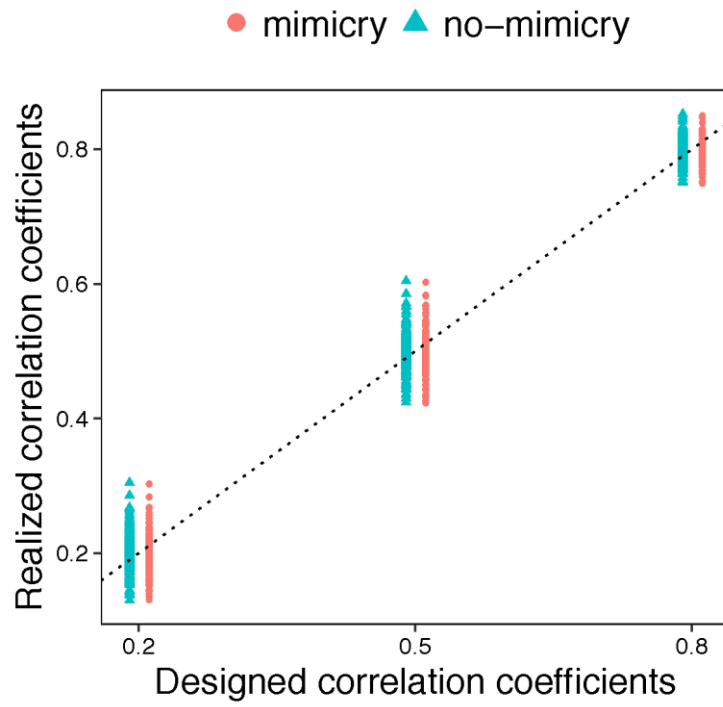
Supplementary Fig. 3 | The distribution of the maximum real part of the eigenvalues of the community matrix of constructed communities. Numbers in the shaded area indicate the identity of the modules in Supplementary Fig. 1.



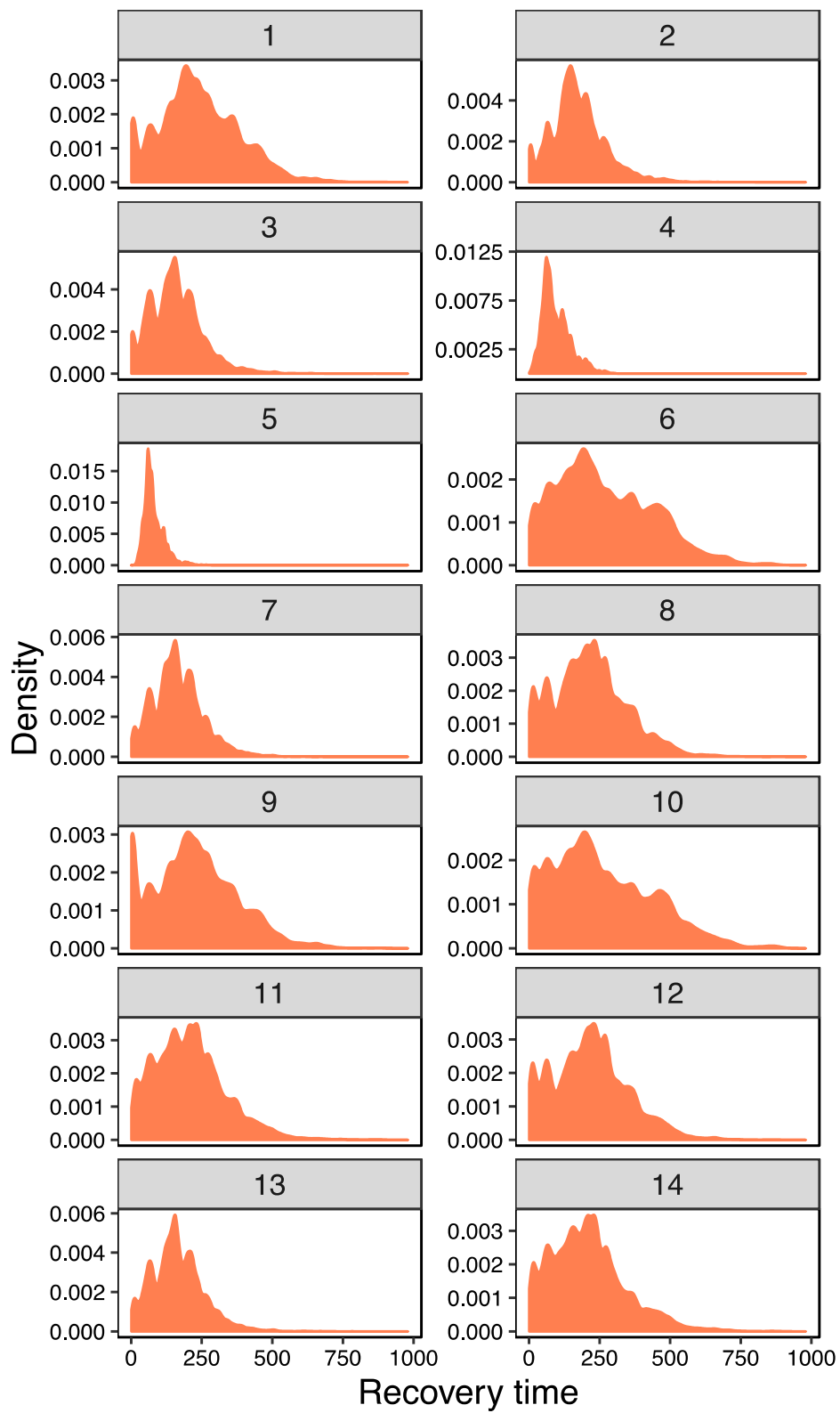
Supplementary Fig. 4 | The equilibrium density of each species in our simulated communities. Numbers in the shaded area indicates the identity of the modules in Supplementary Fig. 1. Numbers along the x-axis represent the species identity that is marked on the module node.



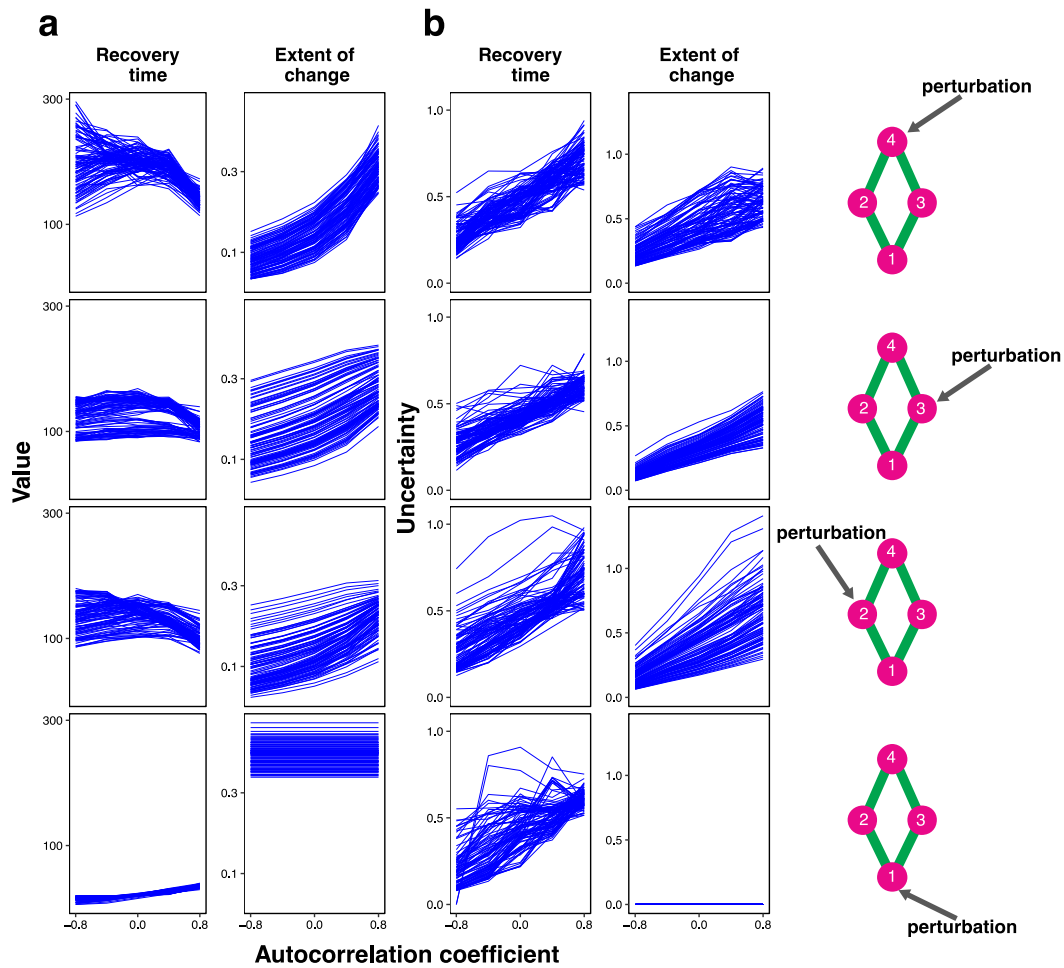
Supplementary Fig. 5 | The realized temporal autocorrelation of the environmental stochasticity time series generated by the autoregressive method (no-mimicry) and that generated by spectral mimicry (mimicry). The dashed line is the identity line where $x = y$.



Supplementary Fig. 6 | The realized species response correlation generated by the autoregressive method (no-mimicry) and that generated by spectral mimicry (mimicry). The dashed line is the identity line where $x = y$.



Supplementary Fig. 7 | The distribution of recovery time in our simulated communities.
 Numbers in the shaded area indicates the identity of the modules in Supplementary Fig. 1.



1
2
3
4
5
6
7
8
9
10
11
12
13

Supplementary Fig. 8 | Sensitivity analysis of the identity of the species receiving perturbations by perturbing each species of the diamond module in isolation. The grey arrows on the right point to the species receiving the pulse perturbation. Because variability was calculated from unperturbed timeseries, it is not included here. **a.** General stability responses and **b.** uncertainty of those responses to changes in environmental autocorrelation. Individual lines in **a.** and **b.** correspond, respectively, to the mean and coefficient of variation in the response across 50 noise replicates for each of the 100 communities of the diamond module. All responses in **a.** are inversely related to stability (*i.e.* stability decreases from the bottom to the top of the y-axis in every case). For this illustrative example, the correlation of species responses to environmental fluctuations was set to 0.2.